Critical state analysis of two compacted filtered iron ore tailings with different gradings and mineralogy at different stages of treatment

Nilo Cesar Consoli[1]; João Paulo Sousa Silva[2]; Alexia Cindy Wagner[3]; João Vítor de Azambuja Carvalho[4]; Beatrice Anne Baudet[5]; Matthew Richard Coop[6]; Hugo Carlos Scheuermann Filho[7]; Inácio Carvalho[8]; Gustavo Marçal de Sousa[9]; and Pedro Pazzoto Cacciari[10]

ABSTRACT: Slurry tailings storage in large impoundments has been largely used worldwide for a long time, as their cost is very competitive. However, recent disasters have brought to light the need to better comprehend the mechanics of the materials stored and to search for disposal alternatives to overcome the drawbacks. One possibility is the filtered tailings disposal (dry stacking) which requires a better understanding of the material's response in a dewatered (through filtration) and compacted condition. This paper compares two tailings from the same beneficiation (treatment) plant with different gradings and mineralogy, related to the beneficial processes they undergo. A series of triaxial tests comprising isotropic compression without shearing specimens, as well as isotropic compression followed by drained (CID) and undrained (CIU) shearing, and K-compression followed by undrained (CKU) shearing specimens were conducted over a range of confining pressures and initial compaction degrees. The experimental program allowed the evaluation of convergence for Normal Compression Lines (NCLs) and the analysis under the light of critical state soil mechanics for the stress-strain response of the tested materials. The research outcomes show that changes in iron ore tailings gradings due to different production processes and the use of different compaction degrees had an influence on its behavior (compression and shearing) at lower stress levels, while at higher stresses levels, this difference is erased and there is a convergence for unique and parallels NCL and CSL on $v - \ln p'$ plane with a spacing of 2.71. On the p'-q plane both tailings showed a unique and similar CSL.

Keywords: Tailings, iron ore tailings, compacted filtered tailings disposal, dry stacking, critical state soil mechanics, static liquefaction.

---

[1] Professor of Civil Engineering, Graduate Program in Civil Engineering, Universidade Federal do Rio Grande do Sul, Porto Alegre, RS, 90035-190, Brazil. E-mail: consoli@ufrgs.br (ORCID: **0000-0002-6408-451X**) **(corresponding author)**

[2] Expert Engineer, Exploration and Mineral Projects - Mineral Development Centre, VALE S.A., Santa Luzia, MG, 33040-900, Brazil. E-mail: joao.paulo.silva@vale.com (ORCID: **0000-0001-9829-880X**)

[3] Ph.D. student, Graduate Program in Civil Engineering, Universidade Federal do Rio Grande do Sul, Porto Alegre, RS, 90035-190, Brazil. E-mail: alexia-wagner@hotmail.com (ORCID: **0000-0002-7351-3910**)

[4] M.Sc. student, Graduate Program in Civil Engineering, Universidade Federal do Rio Grande do Sul, Porto Alegre, RS, 90035-190, Brazil. E-mail: azambuja.jvc@gmail.com (ORCID: **0000-0002-7555-5022**)

[5] Associate Professor, Department of Civil, Environmental & Geomatic Engineering, Faculty of Engineering Science, University College London, London, United Kingdom. E-mail: b.baudet@ucl.ac.uk (ORCID: **0000-0003-0318-6640**)

[6] Professor of Geotechnics, Department of Civil, Environmental & Geomatic Engineering, Faculty of Engineering Science, University College London, London, United Kingdom. E-mail: m.coop@ucl.ac.uk (ORCID: **0000-0002-3301-552X**)

[7] Research Fellow, Graduate Program in Civil Engineering, Universidade Federal do Rio Grande do Sul, Porto Alegre, RS, 90035-190, Brazil. E-mail: hugocsf@ufrgs.br (ORCID: **0000-0001-7590-896X**)

[8] Manager, Exploration and Mineral Projects - Mineral Development Centre, VALE S.A., Santa Luzia, MG, 33040-900, Brazil. E-mail: inacio.carvalho@vale.com

[9] Expert Engineer, Geotechnical Project Management, VALE S.A., Nova Lima, MG, 34006-270, Brazil. E-mail: gustavo.marcal@vale.com

[10] Assistant Professor, Department of Civil, Geological and Mining Engineering, Polytechnique Montreal, Quebec, H3C 3A7, Canada. Formerly Expert Engineer, Exploration and Mineral Projects - Mineral Development Centre, VALE S.A., Santa Luzia, MG, 33040-900, Brazil. E-mail: pedro.cacciari@polymtl.ca

1 Introduction

Brazil is one of the largest iron ore producers in the world, with approximately 338 million metric tons produced in 2020 [1]. Consequently, by-products of the extraction and processing of these materials are generated and must be correctly treated and disposed to minimize environmental and failure risks. Tailings are a byproduct of the mining industry, consisting of the material left after extraction of the valuable fractions from ores.

The physical and chemical characteristics of tailings vary a lot due to the different compositions of the parent ores, as well as the different extraction processes they undergo [2]. Commonly, tailings present an aqueous slurry form comprising disintegrated rocks, chemicals, and elevated amounts of water [3, 4]. These characteristics facilitate their disposal in large impoundments designated as tailings dams. Nevertheless, elevated risks are associated to the operation and maintenance of such structures, since the tailings are routinely found saturated and at a loose state [5–7].

Worldwide, there have been over 240 major Tailings Storage Facilities (TSF) failures since 1960, being at least 5 catastrophic incidents in the last years. Amongst them, were cases such as Mariana and Brumadinho in Brazil, which were upstream tailings dams and represented the biggest disasters in Brazil's history in terms of environmental pollution and loss of lives, respectively [8]. For these reasons, the Brazilian legislation has been revised, indicating an urgent need to safely decommission upstream tailings dams because these are the most challenging structures to operate in the mining industry. Some of these structures are likely to be subject to piping, collapse, and flow failure and should be monitored carefully [2, 9].

Other methods of disposal are being developed and proposed to overcome the risks involved in such structures. In this regard, the filtered tailings disposal by dry stacking appears as an alternative to the traditional disposal of tailings in impoundments and, as well, might be an option for usage in the de-characterization process of an existing dam [10, 11]. Filtering of tailings can take place using pressure or vacuum force. The filtered tailings are transported by conveyor or truck and then placed, spread, and compacted to form an unsaturated, dense, and stable tailings stack requiring no dam for retention [12].

In order to safely design the different disposal methods available and prevent failures, Santamarina et al. [13] synthesized key concepts such as enhanced physical understanding, effective engineering and management, and enforcement of regulations. Associated to the design, usually, are the development and use of advanced constitutive models, mostly based on a critical state framework.

Studies on liquefaction [14–17] have examined the influence of the fines content of the soil on its behavior in the critical state, especially in relation to the shape and location of the CSL (Critical State Line) in the v - ln p' plane. However, the findings of different authors seem contradictory because of the lack of research covering different types of soils. Thevanayagam et al. [18] found that the shape of CSL for different gradings remained similar, but as fines were added, the location of the CSL initially moved downwards in the v - ln p' plane and then moved upwards again. The authors defined as the "threshold fines content" the grading that gave the lowest location on the CSL plane. The studies of Carrera et al. [14], who tested tailings from the Stava disaster, agreed with the findings of Thevanayagam et al. [18]. Torrez-Cruz and Santamarina [19] compiled published data and new experimental results and concluded that the intercept of the CSL on v - ln p' plane as well as the value of e_{min} (minimum void ratio) are lowest for mixtures with intermediate fines content (FC), typically FC ≈ 30%.

The amount of non-plastic fines has also been found to influence the compression behavior, with most of the existing research on one-dimensional compression up to conventional stress and some include high-stress levels. Carrera et al. [14] have found that the location of the 1D-NCL moved downwards and reduced its inclination in the e - $log(\sigma'_v)$ plane as the fine content was increased, and the trend reversed for contents higher than 50–70%. Li and Coop [20] identified unique 1D-NCLs for each of the three iron tailings from Panzihua, China, that they tested. Also, the authors noted that the finest material reached a 1D-NCL much earlier than the coarser materials. Several studies have highlighted the difficulty of achieving unique NCLs (Normal Compression Lines) and CSLs for samples created at different initial conditions for both natural soils and tailings [2, 20–24] which limits the characterization of these materials under the critical state framework, indicating a dependence of the behavior on the initial specific volume termed "transitional behavior".

In this work, detailed laboratory tests were designed to investigate two iron ore tailings (IOT) from the same tailings facility with different gradings, related to the beneficial (treatment) processes they undergo. The two tailings present different proportions of sand and silt, as a result of the different processing methods they were subjected to. Isotropic compression tests were carried out to high pressures (120 MPa) in specimens with different initial densities to study the effect of grading and the initial void ratio on the compressibility of the tailings and the convergence of NCLs over a broad spectrum of pressures. Particle breakage after isotropic compression tests was also evaluated, considering the different tailings and initial void ratios. The shearing response of the materials was assessed through compression drained (CID) and undrained (CIU and CKU) triaxial tests conducted over a wide range of confining pressures (σ'_3 ranging from 50 to 2,400 kPa) and specific volumes ($v \approx 1.50$ to 2.10) to identify the CSLs for each grading, and to examine liquefaction potential relative to the location of these lines. Bender elements were used to analyze the stiffness of tailings with different gradings and degrees of compaction. The effect of the compactness and a possible occurrence of transitional behavior was also investigated on the compression and shearing as the specimens were compacted to different initial specific volume values (v_0).

2 Experimental program

The experimental program comprised the physical characterization of both iron ore tailings and the evaluation of their compression and shear behavior. A total of 50 triaxial compression tests were conducted, with different initial densities, and 3 isotropic compression tests were performed for each material. Also, bender elements were used in 4 tests to evaluate the small strain stiffness of the tailings.

2.1 Materials

The iron ore tailings (IOT) studied herein is from Quadrilátero Ferrífero (QF), in the central region of the state of Minas Gerais in Brazil. This region produces approximately 200 million tons of iron ore per year and is responsible for approximately 65% of all Brazilian iron ore production. Ore processing includes simple crushing and screening methods to more sophisticated processes to upgrade the ore quality. After the screening stage, the fine material, with gradation below the sinter feed (particles diameters from 0.15 to 6.3 mm), moves on to a desliming stage through a sequence of hydro-cyclone batteries to remove the finer material (slime tailings (S)). After this stage, the slimes tailings (S) are stored, and the remaining material moves on to the reverse cationic flotation process, which isolates the fine-grained ore (pellet feed), and results in the flotation tailings (F) that are also stored.

The iron ore tailings analyzed in this study are of the slime type (S) and flotation type (F), obtained according to the procedure described above, and were collected in a disturbed state from a mine at QF. The tailings samples were collected directly from the storage facilities. The fine tailings (slimes) were excavated into the dam with the aid of a dragline. In contrast, the tailings from the flotation stage were collected from the pile of filtered dry tailings. X-ray diffraction analysis shows 54.8% of quartz, 42.3% of hematite and 2.9% of kaolinite for the slimes tailings (S) and 98.3% of quartz and 1.7% hematite for the flotation tailings (F). Table 1 summarizes the main physical characteristics of both tailings, whereas Fig. 1 portrays the grain size distributions. The particle-size distribution (PSD) was obtained following the ASTM D7928 [25] standard. The Atterberg limits and the specific gravity were evaluated, respectively, according to ASTM D4318 [26] and ASTM D854 [27]. The minimum (e_{min}) and maximum (e_{max}) void ratios were evaluated in agreement with ASTM D4254 [28] and ASTM D4253 [29] respectively. The compaction characteristics were assessed using both the standard and modified efforts in agreement to ASTM D698 [30] and ASTM D1557 [31]and these results are presented in Fig. 2. The slime tailings (S) are classified as low plasticity silt (ML) and the flotation tailings (F) are classified as silty sand (SM) in accordance with the Unified Soil Classification System [32].

Table 1 - Physical properties of iron ore tailings.

Parameters	**S**	**F**
Specific gravity – G_s	4.02	2.83
Gravel (%)	0.00	0.00
Coarse sand (%)	0.00	0.00
Medium sand (%)	1.39	0.40
Fine sand (%)	12.42	61.00
Silt (%)	79.93	35.12
Clay (%)	6.26	3.48
w_L (%)	-	-
PI (%)	Nonplastic	Nonplastic
Coefficient of uniformity	9.0	5.75
Coefficient of curvature	2.15	1.57
ASTM-USCS Classification	ML	SM
Maximum void ratio – e_{min}	0.565	0.503
Minimum void ratio – e_{max}	1.087	1.078
Optimum water content at standard effort – w_{opt} (%)	12.20	14.20
Maximum dry density at standard effort – γ_{dmax} (kN/m^3)	25.09	17.28
Optimum water content at modified effort – w_{opt} (%)	10.00	12.80
Maximum dry density at modified effort – γ_{dmax} (kN/m^3)	26.55	18.23

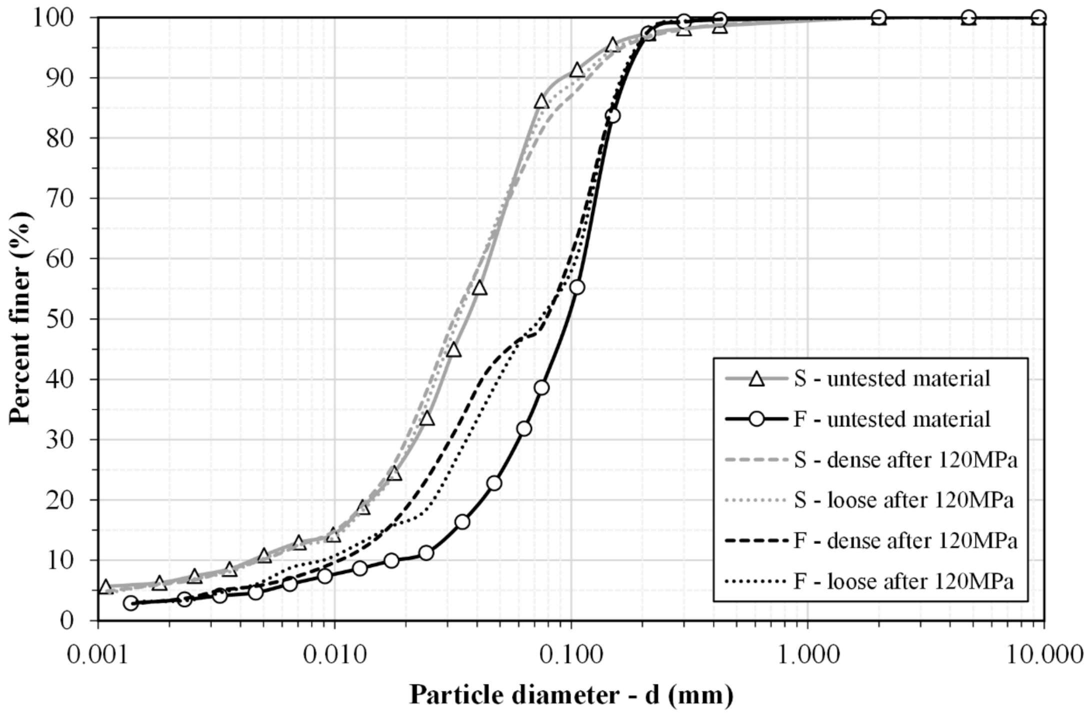

Figure 1 – Particle size distribution of the iron ore tailings.

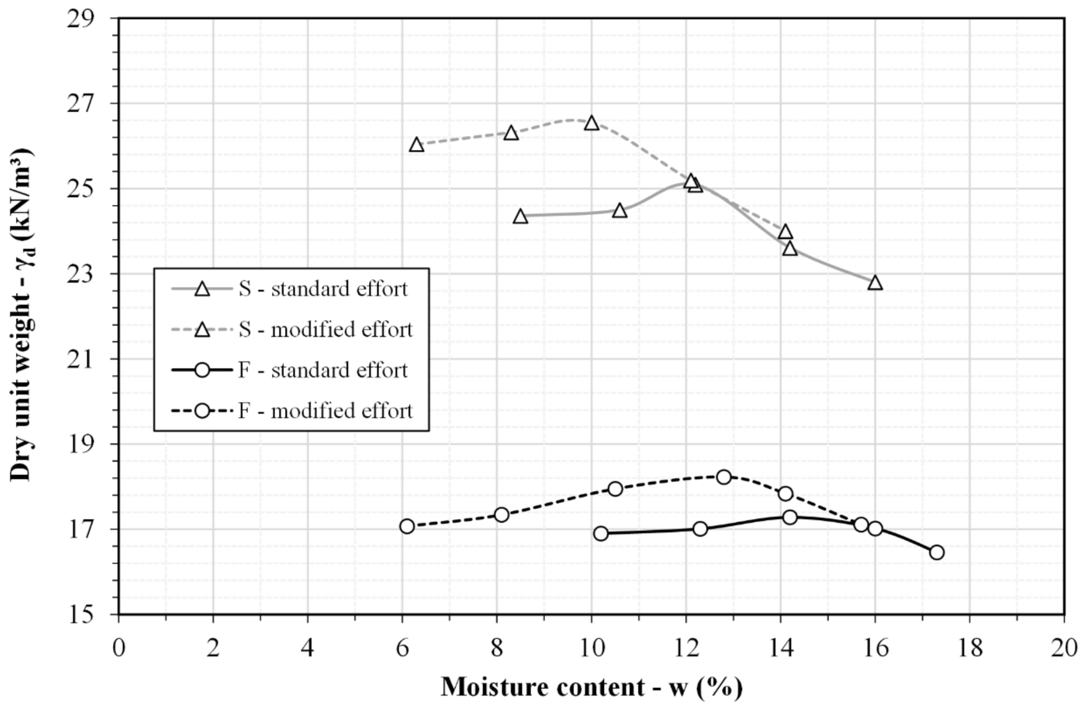

Figure 2 – Compaction characteristics of the iron ore tailings.

As described above, differences in the physical properties of the two tailings are associated with their production process. The slime tailings have finer particles (86.2% passing sieve 0.075mm) and considerably higher specific gravity due to the presence of particles with high iron content. These tailings are retrieved at the initial stage of treatment, before the flotation process. Thus, flotation tailings are coarser (38.6% passing sieve 0.075mm) because they are obtained after desliming and have a lower specific gravity due to the recovery of pellet feed at this stage. These characteristics also influence the compaction behavior of the materials since the dry unit weight is much higher for the slime tailings due to its high specific gravity.

2.2 Methods

A total of 25 triaxial tests were carried out for flotation tailings and 25 for slime tailings. For both materials, different stress paths were conducted, which allowed for assessing the stress-strain behavior and liquefaction potential, as well as analyzing the results under the critical state framework.

2.2.1 Isotropic Compression Testing

Isotropic compression tests were completed for loose and dense states of each material, totalizing six tests. The specimens were prepared by moist tamping at three different molding specific volumes for each tailings (υ = 1.65, 1.73 and 1.88 for flotation specimens and υ = 1.67, 1.73 and 1.79 for slimes specimens). For the isotropic compression tests, specimens with 50 mm in diameter and 100 mm in height were used. The maximum isotropic stress applied to the specimens was about 120 MPa.

2.2.2 Triaxial Compression Testing

Triaxial tests were carried out following the determinations of ASTM D7181 [33] for drained tests and ASTM D4767[34] for undrained tests. Cylindrical specimens having 70mm in diameter and 140mm in height were molded through moist tamping [35, 36]. The specimens were compacted to four degrees of compaction relative to the standard effort (i.e., 75% - 450 kN-m/m^3 (75N), 85% - 510 kN-m/m^3 (85N), 95% - 570 kN-m/m^3 (95N), and 100% - 600 kN-m/m^3(100N)) and one degree relative to the modified effort (i.e., 100% - 2,700 kN-m/m^3 (100M)). This spectrum was defined aiming to reproduce feasible levels of compactness for use in dry stacking and to investigate the occurrence of "transitional behavior". Such occurrence would imply the dependence of the location of both the normal compression line and the critical state line on the initial specific volume [21, 23]. In other words, a transitional geomaterial would present multiple NCLs or CSLs, depending on the initial degree of compaction that would result in fabric differences that would not be fully erased during compression and/or shear. Based on the compaction curve results (Fig. 2) moisture contents (w) between 13% and 15% were chosen for flotation tailings (F) and 10% and 13% to slime tailings (S). Steel split molds were used and manual compaction in six layers of equivalent height was completed.

For the CID and CIU triaxial tests, the specimens were isotropically consolidated to a range of initial effective confining pressures (σ'_3 = 50 kPa to σ'_3 = 2,400 kPa). For the CKU tests, the consolidation stresses were gradually applied by servo-controlled adjustment of deviatoric load and cell pressure to the target coefficient of lateral pressure ($K = \sigma'_h/\sigma'_v$) of 0.70. Oversized end platens and lubricated “free-ends” were used to minimize the effects of end friction during the triaxial tests. After consolidation, the specimens were sheared either drained or undrained at a constant rate of 1.5% per hour for a total axial strain of approximately 30%. Pore-pressures or volume change, vertical load, and axial displacement were recorded continuously throughout the tests. At the end of the tests, the specimens were frozen, allowing the determination of the final water content and the accurate measurement of the initial and final void ratios. Table 2 summarizes the data relative to the triaxial tests conducted on the flotation tailings and Table 3 summarizes the data relative to the triaxial tests conducted on slime tailings. The notation used to identify each test is also presented in the tables.

Table 2 – Summary of triaxial compression tests data for flotation tailings.

Identification	Soil	Type	Compaction energy	v at molding	v at shear	p'_0 (kPa)
1F	F	CID	75N	2.09	1.93	150
2F	F	CID	75N	2.08	1.90	300
3F	F	CID	75N	2.10	1.86	600
4F	F	CID	75N	2.11	1.83	1200
5F	F	CID	75N	2.10	1.80	2400
6F	F	CID	85N	1.90	1.89	100
7F	F	CID	85N	1.90	1.86	300
8F	F	CID	95N	1.72	1.74	100
9F	F	CID	95N	1.72	1.73	300
10F	F	CID	100N	1.65	1.67	50
11F	F	CID	100N	1.63	1.66	100
12F	F	CID	100M	1.57	1.59	200
13F	F	CID	100M	1.57	1.61	400
14F	F	CID	100M	1.57	1.58	1200
15F	F	CIU	75N	2.13	1.98	100
16F	F	CIU	75N	2.12	1.94	200

17F	F	CIU	75N	2.10	1.91	400
18F	F	CIU	75N	2.11	1.84	800
19F	F	CIU	75N	2.07	1.81	1600
20F	F	CKU	75N	2.08	1.89	400
21F	F	CKU	75N	2.09	1.86	800
22F	F	CKU	75N	2.09	1.80	1600
23F	F	CKU	85N	1.91	1.85	800
24F	F	CKU	95N	1.71	1.72	800
25F	F	CKU	95N	1.71	1.71	1600

Table 3 – Summary of triaxial compression tests data for slime tailings.

Identification	Soil	Type	Compaction energy	v at molding	v at shear	p'_0 (kPa)
1S	S	CID	75N	2.09	1.82	150
2S	S	CID	75N	2.09	1.81	300
3S	S	CID	75N	2.11	1.78	600
4S	S	CID	75N	2.09	1.74	1200
5S	S	CID	75N	2.11	1.70	2400
6S	S	CID	85N	1.88	1.82	100
7S	S	CID	85N	1.88	1.81	300
8S	S	CID	95N	1.68	1.7	100
9S	S	CID	95N	1.67	1.69	300
10S	S	CID	100N	1.61	1.64	50
11S	S	CID	100N	1.61	1.63	100
12S	S	CID	100M	1.54	1.56	200
13S	S	CID	100M	1.53	1.55	400
14S	S	CID	100M	1.53	1.54	1200
15S	S	CIU	75N	2.05	1.86	100
16S	S	CIU	75N	2.10	1.83	200
17S	S	CIU	75N	2.11	1.79	400
18S	S	CIU	75N	2.10	1.75	800
19S	S	CIU	75N	2.07	1.70	1600
20S	S	CKU	75N	2.11	1.80	400
21S	S	CKU	75N	2.11	1.76	800
22S	S	CKU	75N	2.09	1.71	1600
23S	S	CKU	85N	1.86	1.77	800
24S	S	CKU	95N	1.68	1.69	800
25S	S	CKU	95N	1.67	1.65	1600

2.2.3 Bender Elements

Four tests (4F, 14F, 5S, and 14S) were isotropically consolidated incrementally in the following stages approximately: 50 kPa, 150 kPa, 300 kPa, 600 kPa, and 1,200 kPa. In each stage bender elements (BE) tests were completed. The specimens were then unloaded incrementally to approximately 600 kPa, 300 kPa, and 150 kPa and the BE tests were repeated in each unloading stage, after which the specimens were reloaded to the target confining pressures. The remaining specimens were all isotropically consolidated in a single stage to the target pressures.

3 Results and discussion

3.1 Compression Behavior

3.1.1 Isotropic compression

The compression curves obtained for the two tailings are shown in Fig. 3. The convergence of the compression curves from different initial v_0 is very slow, so that even at the maximum stress level of about 120 MPa the curves have still not quite converged to a unique NCL. This suggests that even for a very large tailings stack of 300 m height, the compression even at the base would not cause a NCL to be reached.

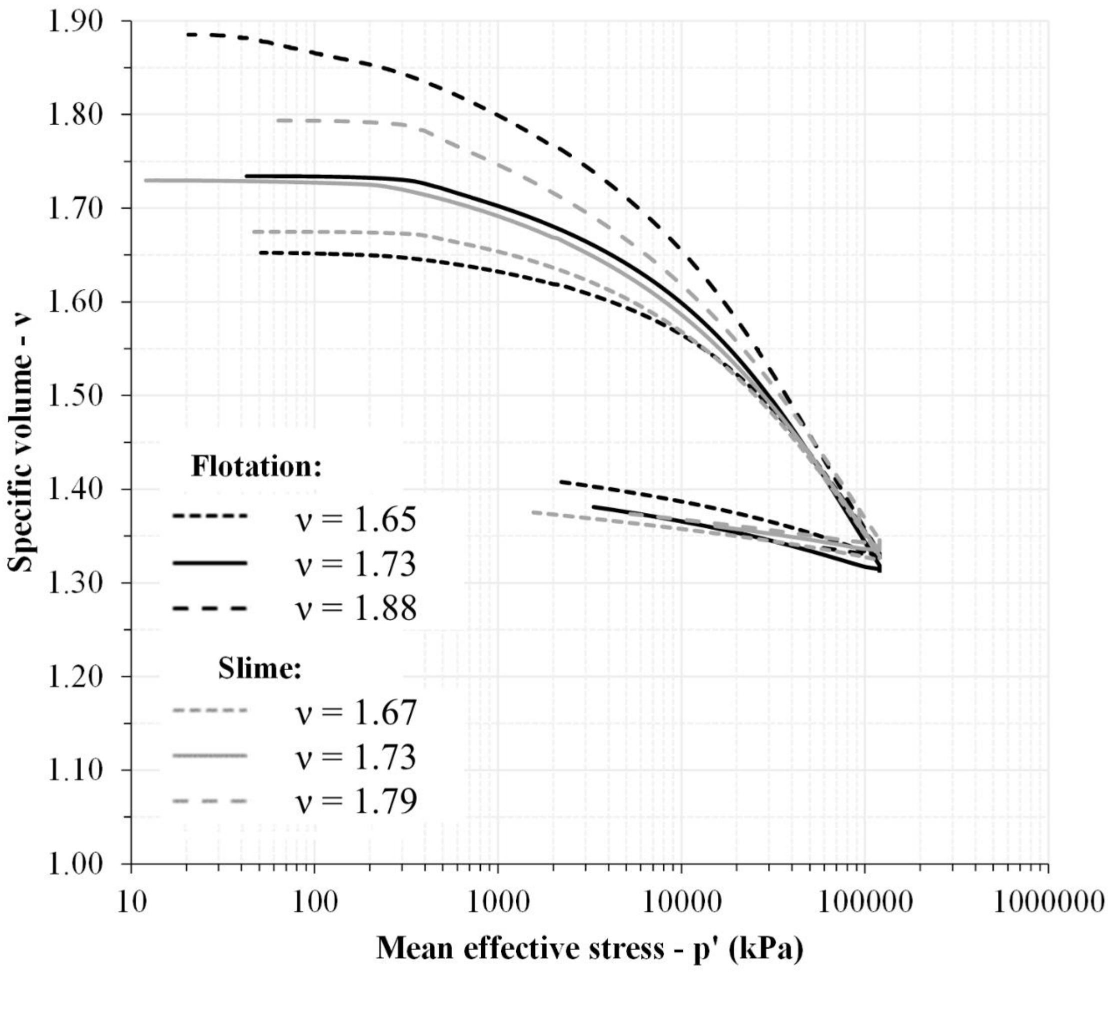

Figure 3 – Isotropic compression results.

This is demonstrated in Figure 3, where all the specimens show the tendency to converge towards the same specific volume at very high pressures (120 MPa). In this regard, a slight change in the response can be roughly identified on the curves at lower stress levels, but a clear yield point could be not identified due to scale reasons. Moreover, the response during the unloading was much stiffer, indicating the occurrence of large plastic deformations. The convergence to the NCL is slower for lower initial specific volumes because the soil experiences much smaller volumetric strains and much higher stresses are therefore needed to reach the NCL. When the initial specific volume is high, the compression curves tend to converge more easily as the volumetric strains are larger.

It is also noted that the two tailings with different gradings tended to converge to exactly the same NCL. For low stresses, the compression behavior of both tailings is also very similar, with the finer material being slightly more compressible, but as the stresses increase, the compressibility of the samples seems to be independent of fines content and mineralogy. As will be discussed later, the flotation tailings underwent particle breakage during compression but the slimes did not, which suggests that the breakage that occurred in the flotation tailings did not control yielding or convergence to the NCL.

Both studied tailings can be called well-graded, their coefficients of uniformity of 9.0 for slime tailings and 5.75 for flotation tailings are larger and their coefficients of curvature of 2.15 for slime tailings and 1.57 for flotation tailings are in between 1 and 3 [37]. Several studies have been reported in the literature on the compressive behavior of granular soils, the majority being carried out in uniformly graded sands. Authors such as Nakata et al. [38] and McDowell [39] performed one-dimensional compression tests on uniformly graded samples of silica sand and showed that for a given void ratio, the yield stress depends on the particle size and increases with the decrease in particle size. They also noted that the compression index after the yield was independent of particle size.

Looking at the previous literature [2, 14, 20, 40] it is also possible to find other granular materials with different fines content converging to a unique NCL (although in some cases it has not been fully discussed), especially other tailings and sand-silt mixtures. Altuhafi and Coop [40] indicated that uniformity has an important role in compressibility and the location of the yield point in compression curves. The authors studied sands with distinct mineralogy in different gradings (uniform to well-graded) in one-dimensional compression. The sands tested up to 107 MPa showed different compression indexes for different initial gradings; however, it is possible to notice a tendency of convergence to the same specific volume at higher stresses for the two materials tested herein.

Carrera et al. [14]performed oedometer tests on the Stava sand and silt mixed at different percentages with a maximum applied load of approximately 14 MPa. The authors found that the 1D-NCL moves downwards, and the compression index decreases as the silt content increases, with an inversion in the tendency at larger silt contents. The stresses achieved by the authors were significantly lower than those of the present work and from the tendency of the curves is possible that mixtures with different gradings could converge to the same NCL for higher stresses.

Li and Coop [20] found that the compression index decreases with the increasing fines content, which was attributed to a better filling of the voids by the finer particles. The authors identified a unique one-dimensional normal compression line for each iron tailings grading studied, considering a maximum vertical stress of 20 MPa. The convergence of the NCLs for the three gradings studied was not observed for the tested stress level, although two of them show some tendency to converge at very high stresses.

Li et al. [2] studied a silty gold tailings and compared it with the coarser gold tailings studied by Bedin et al. [41]. By comparing the one-dimensional compression behavior of both tailings until 20 MPa, it can be seen that the normal compression lines were in very similar locations, despite the distinct initial gradings.

3.1.2 Particle Breakage

It is well known that granular materials may experience particle breakage during isotropic compression to high mean effective stresses. The evolution of particle breakage during the compression of granular soils and its influence on soil behavior has long been investigated [39, 40, 42–48]. In granular materials, particle breakage has been usually associated with yielding [43]. To investigate the occurrence of particle breakage, the grain size distribution was evaluated for two specimens of each tailings type (loose and dense) after being tested under isotropic stress at 120 MPa. The aim was to examine the effects of particle packing on the tailings' behavior, considering different initial gradings and densities.

The results are shown in Fig. 1 compared to the original grain size distributions. Also, the relative breakage B_r defined by Hardin [49] was calculated. It was 0.16 for both densities of flotation tailings and zero for both densities of slime tailings. Observing the curves and the calculated values, there was no significant difference in the particle breakage of the flotation tailings due to differences in the initial densities. This agrees with the findings of Coop and Lee [43] and suggests that a unique relationship between particle breakage and effective stress might exist independently of the initial density. Altuhafi and Coop [40], however, found that there was more breakage for the samples with a higher initial void ratio after compression, although the effect of the initial void ratio on the amount of breakage was less pronounced for some soils.

It is possibly the higher fines content of the slimes that prevents breakage. Similar behavior was found by Li et al. [2], where the coarser tailings of Bedin et al. [41] was subject to particle breakage while the finer was not. The particle size distribution is related to the packing of the specimen. Muir Wood [24, 50] demonstrated by the discrete element method (DEM) that soils with a wider particle size range (well-graded) have greater packing efficiency, resulting in a higher coordination number for larger particles and thus reducing the probability of breakage. Altuhafi and Coop [40] also demonstrated that the packing efficiency, and thus the coordination number, can be increased by increasing the fines content of the sample. By adding fines and changing the grading of different sands, particle breakage decreased until it ceased. In this case, it is unusual, and perhaps a coincidence, that a tailings with breakage and one without converge to exactly the same NCL.

3.1.3 Quantification of convergence

Ponzoni et al. [51] proposed a method to quantify the convergence of the compression curves using an m value. The m value is based on the relation between an initial specific volume ($v_{initial}$) and the specific volume at maximum stresses reached (v_{final}) and is analyzed with at least two initial densities. The authors define that, for soils with fully convergent compression curves, m is equal to 0 (same v_{final} for different $v_{initial}$). In other words, soils existing at initially different v values, but that reach the same (or very similar) v value at the end of compression, present a convergent compressive response and, thus, a single NCL. For soils with perfectly parallel compression curves, m equals 1. This would indicate the existence of a family of parallel compression curves, each one related to the initial specific volume.

Figure 4 shows m values for the two tailings based on the initial specific volume at 100 kPa of mean effective stress (v_{100}) and at the maximum stresses reached (v_{120000}) at 120,000 kPa. Also, m values are presented based on two intermediate stresses, 1,000 kPa (v_{1000}) and 10,000 kPa (v_{10000}). These intermediate stresses were defined as, respectively, a usual limiting stress level in the geotechnical practice and a possible stress level for application in dry stacks. Straight lines were assumed between v_{100} and the different final specific volumes and the *m* values are between 0 and 1 for both tailings. The results in Fig. 4 indicate again that the compression curves of the two materials are very similar, as the differences between both are smaller than the likely accuracy of the void ratios measured. The *m* values obtained for the three pressures ranges were very similar for both tailings regardless of the gradings, mineralogy and particle breakage. For this reason, the points from the compression curves of the different tailings were fed by a unique *m* value.

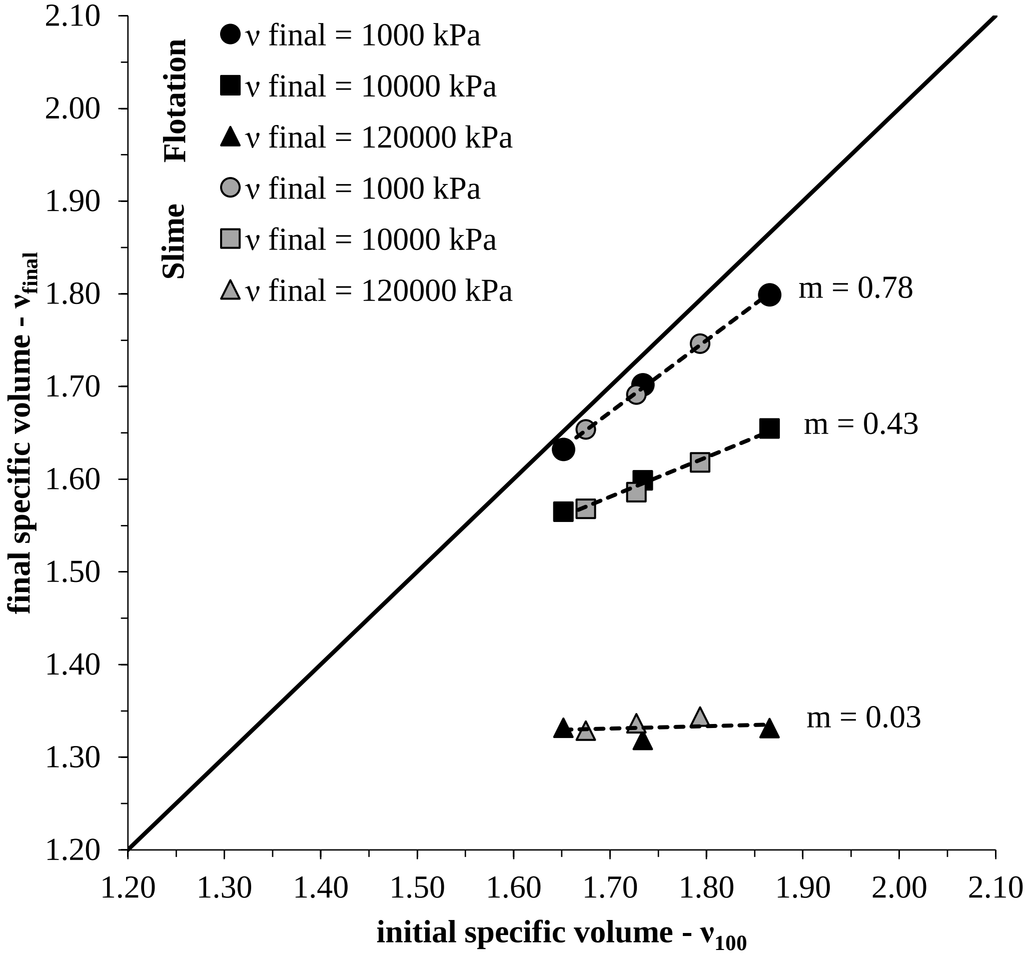

Figure 4 – Convergence lines in isotropic compression.

The *m* value that is not 0 indicates that the initial fabric is still not quite erased for the maximum stress applied. So, it is possible to conclude that at the usual pressures to 1 MPa the compression curves are very different and suggest a form of transitional behavior (*m* is close to 1). A similar tendency is noted in the pressure of 10 MPa, but a greater convergence tendency is confirmed due to the decrease in *m* (*m* is between 0 and 1). Finally, at the highest stress of 120 MPa, all isotropic curves almost converge (*m* is close to 0).

These results demonstrate the importance of evaluating convergence by considering a stress level compatible with the material tested and its application. The *m* values found for the usual range of stresses applied in dry stacks indicate that the mode of behavior expected in these situations is still dependent on the initial fabric, where the deposition density significantly affects the in-situ volume and compression behavior of the material.

3.2 Shearing Behavior

3.2.1 Stress-strain data

Figure 5 presents the stress-strain responses of the IOT under CID (consolidated isotropically drained) shearing tests. It is observed that the behavior of the two types of tailings was very similar. The loosest specimen types (1F/1S to 7F/7S) show a ductile response accompanied by a fully contractive behavior. On the other hand, specimens molded at the highest compaction degrees (8F/8S to 14F/14S) have a peak strength associated with an initial contractive response followed by a dilatant behavior.

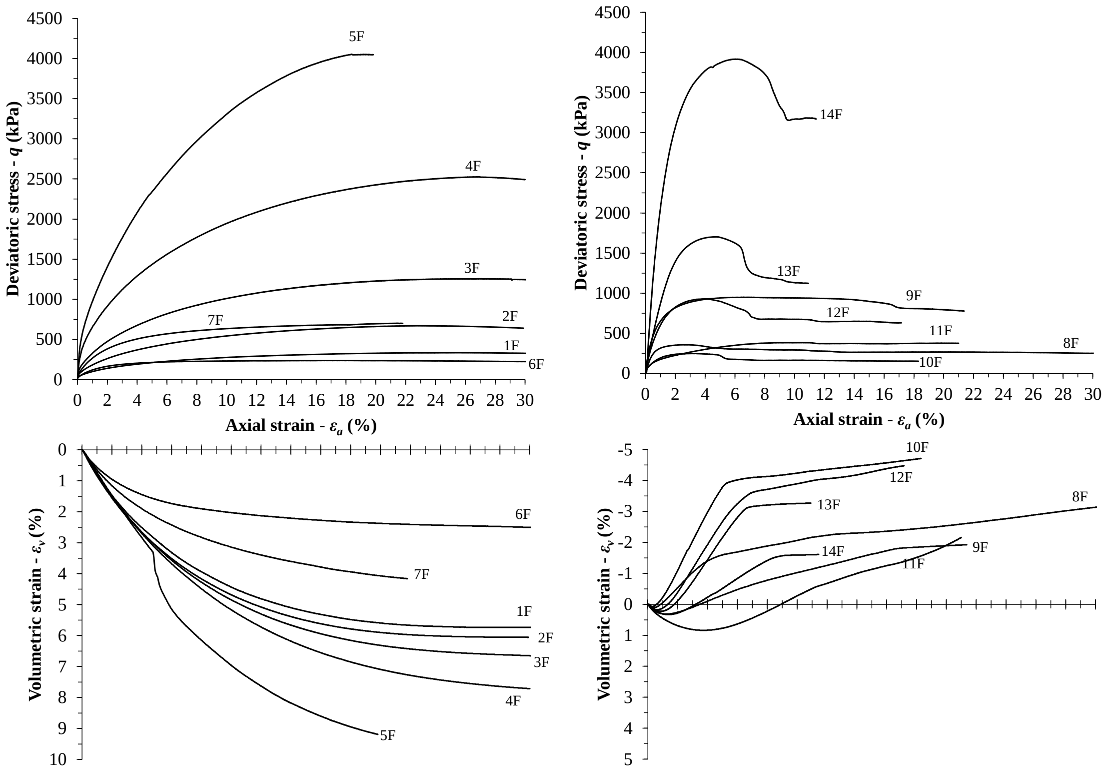

(a)

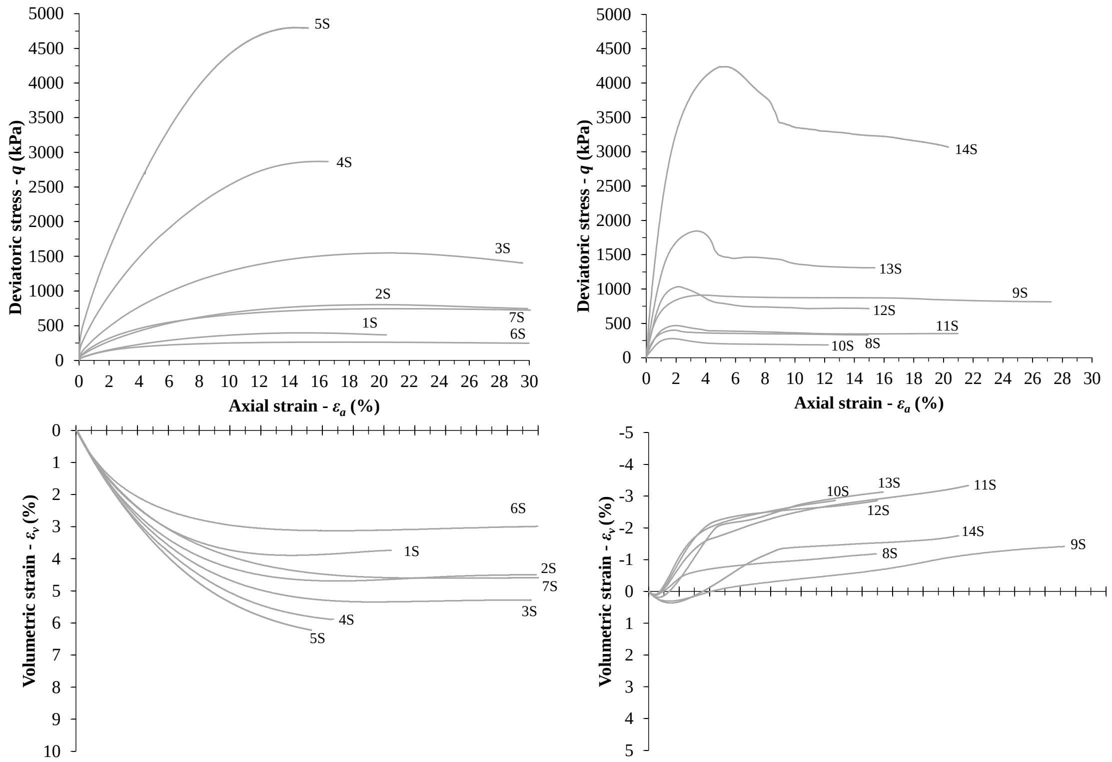

(b)

Figure 5 – Stress-strain results of CID tests for: (a) flotation tailings and (b) slime tailings.

The area correction for the samples was carried out according to La Rochelle et al. [52]. However, it is difficult to obtain real strength values, especially for denser samples due to the localization of strains. In this way, the dense tests were carefully assessed to avoid false conclusions, so dense samples were not used to define the critical state line and only the samples that showed no variation in both volumetric strains and deviatoric stress at large strain levels were considered in the critical state analysis ($\delta\varepsilon_v/\delta\varepsilon_s = \delta\varepsilon_q/\delta\varepsilon_s = 0$).

Figure 6 presents the stress-strain responses of the iron ore tailings isotropically consolidated and sheared under undrained conditions (CIU tests). Unlike the drained tests, the undrained behavior of the two types of tailings presents significant differences, especially concerning the stress-strain response. As all samples were molded in a loose state, a positive change of pore-pressure was generated during shearing. For flotation tailings specimens (Fig. 6a), a substantial loss of strength, accompanied by a strain softening behavior, was observed corresponding to the positive pore-pressure increments registered during shearing. Hence, this has led to static liquefaction or, at least, to susceptibility to it, especially for the specimens sheared at low levels of initial effective confining pressure.

The slime tailings specimens (Fig. 6b) do not show the complete loss of strength, or true liquefaction, although specimens 15S and 16S presented a peak strength followed by strain softening behavior. Tests 17S, 18S, and 19S, which were sheared at higher confining pressures, showed contractive behavior with peak strengths at up to approximately 1% strain followed by a quasi-steady state which lasts for a short range of strains, after which the deviatoric stress increases again with a tendency to dilatant behavior. Li et al. [2] and Li and Coop [20] found similar behavior in undrained shear. The slime tailings were more compressible in the consolidation than the flotation tailings, resulting in greater proximity in relation to the CSL (see Fig. 12) at the beginning of the shearing and, consequently, smaller values of the state parameter [53–55]. As a reason, the loosely compacted slime tailings samples (lying above the CSL) were less contractive during shearing than the corresponding flotation tailings specimens, implying a lesser amount of positive pore-pressure generation during undrained shear [56].

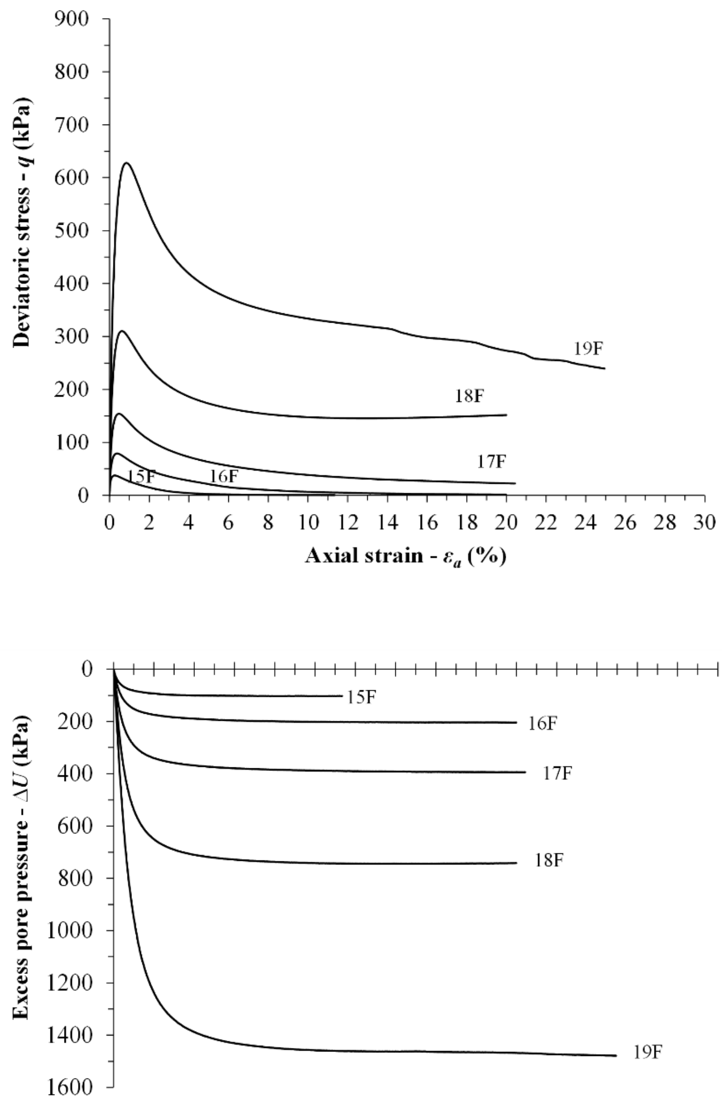
Deviatoric stress - q (kPa)
Axial strain - εa (%)
19F
18F
17F
16F
15F
Excess pore pressure - ΔU (kPa)
15F
16F
17F
18F
19F

(a)

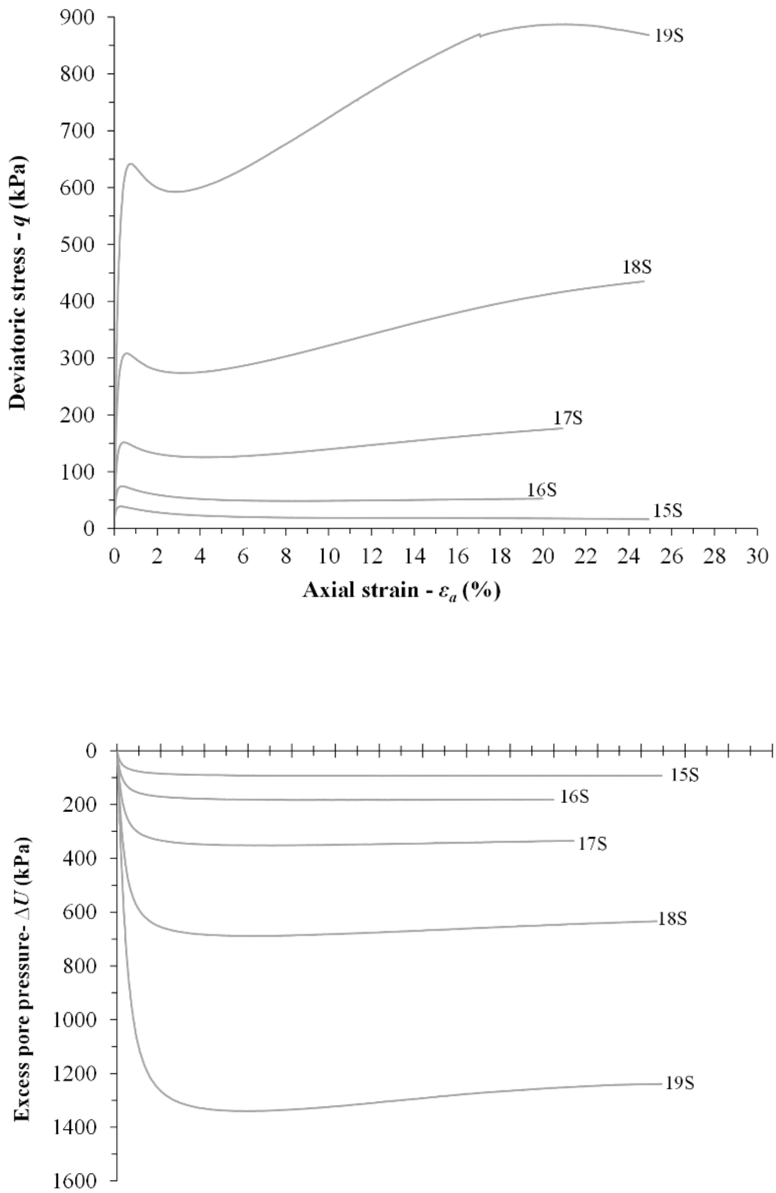

(b)

Figure 6 – Stress-strain results of CIU tests for: (a) flotation tailings and (b) slime tailings.

Figure 7 presents the stress-strain responses of the iron ore tailings K-consolidated and sheared under undrained conditions (CKU tests). It is noted that the K-consolidated specimens' response was similar to the isotropically consolidated specimens. The denser samples have an initial positive change of pore-pressure, followed by a negative pore-pressure generation trend accompanied by a slight peak strength. In general, the looser specimens have a loss of strength, accompanied by a strain-softening behavior, and positive pore-pressure increments were observed during shearing. Strength loss was larger for the flotation tailings specimens, while it was either slight or there was a strain hardening trend for some slime tailings specimens.

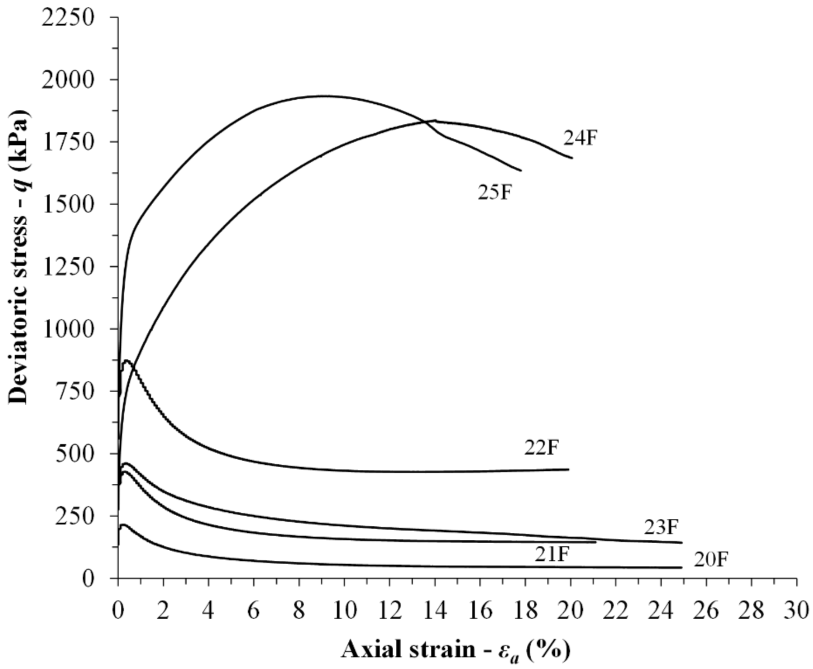

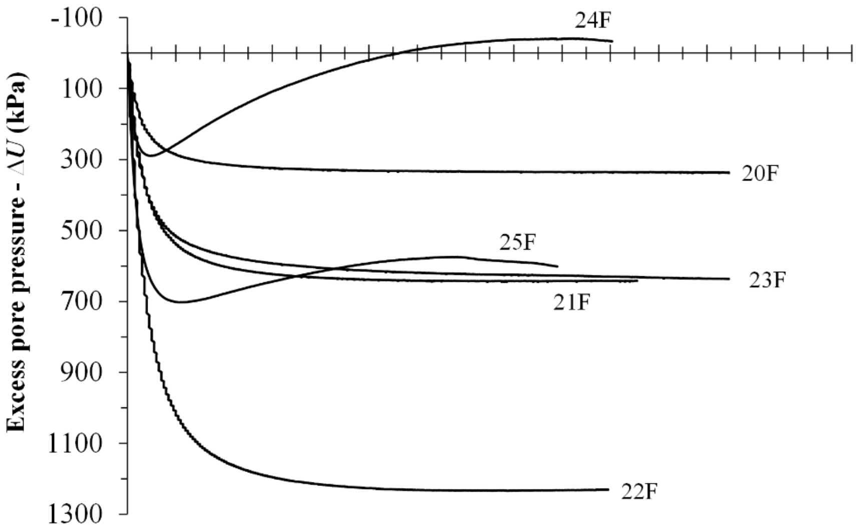

(a)

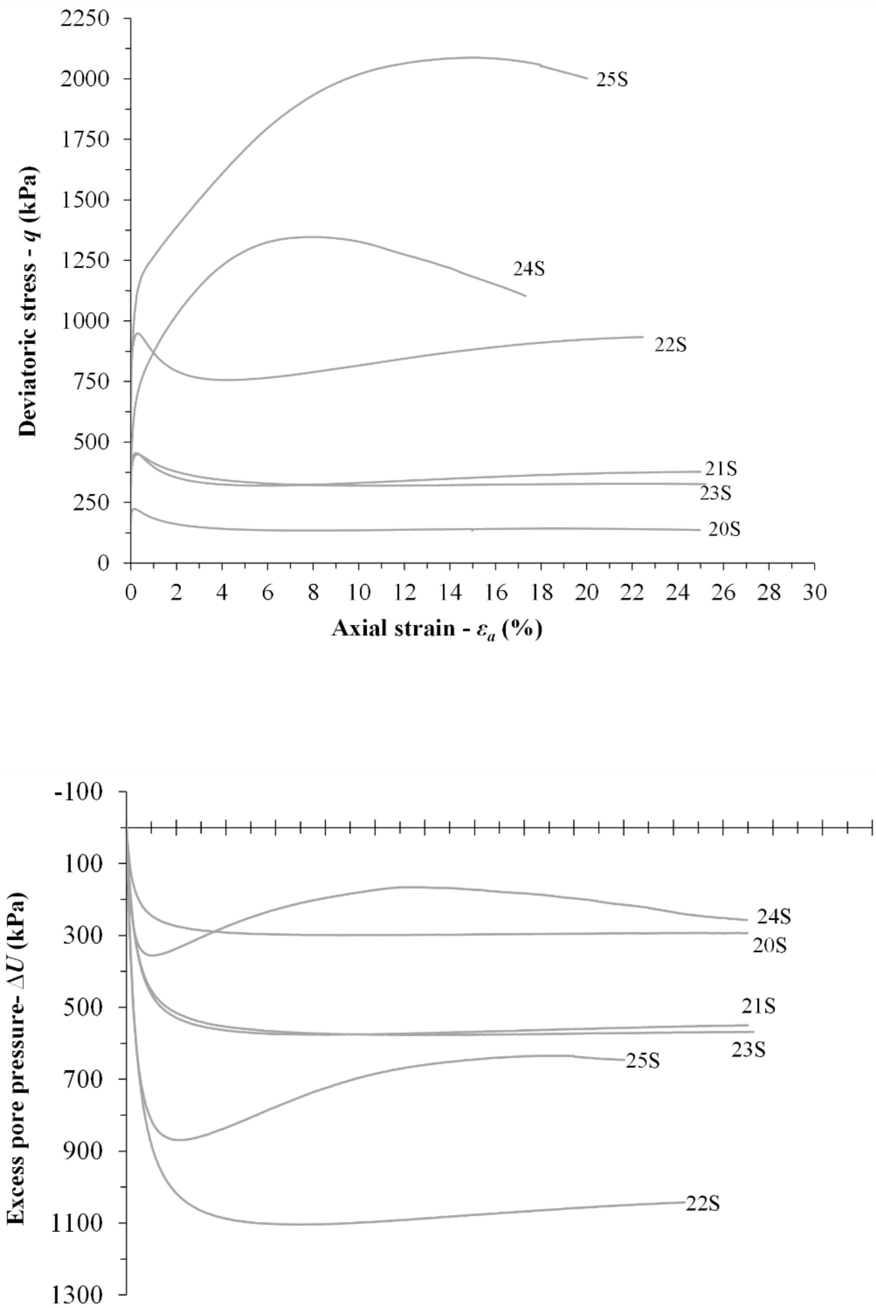

(b)

Figure 7 - Stress-strain results of CKU tests for: (a) flotation tailings and (b) slime tailings.

3.2.2 Elastic shear modulus

Figure 8 presents the elastic shear modulus (G_{max}) determined with BE testing to both tailings studied at different initial states. It is observed that the values of small strain shear modulus are influenced by the effects of initial density and the state of stress. The results agree with the

Hertzian contact theory which, ultimately, states that the small strain stiffness in a porous media is dependent upon the contact area between the constituent particles [57–59]. Hence, G_{max} increases with the decrement in υ which, in turn, decreases owing to the augment of the mean effective stress (*p´*). In this regard, both results fit well a power law with the same exponent equal to 0.55. This suggests that the scalar accounts for the fabric existing differences between the slime and flotation tailings as well as within the samples molded using the same tailings but at different densities (loose and dense). Regarding the two types of tailings, the slime tailings were stiffer, possibly due to the higher fines content and better packing of the specimens, which guarantees a greater contact area between the particles, as well as because of the differences in mineralogy.

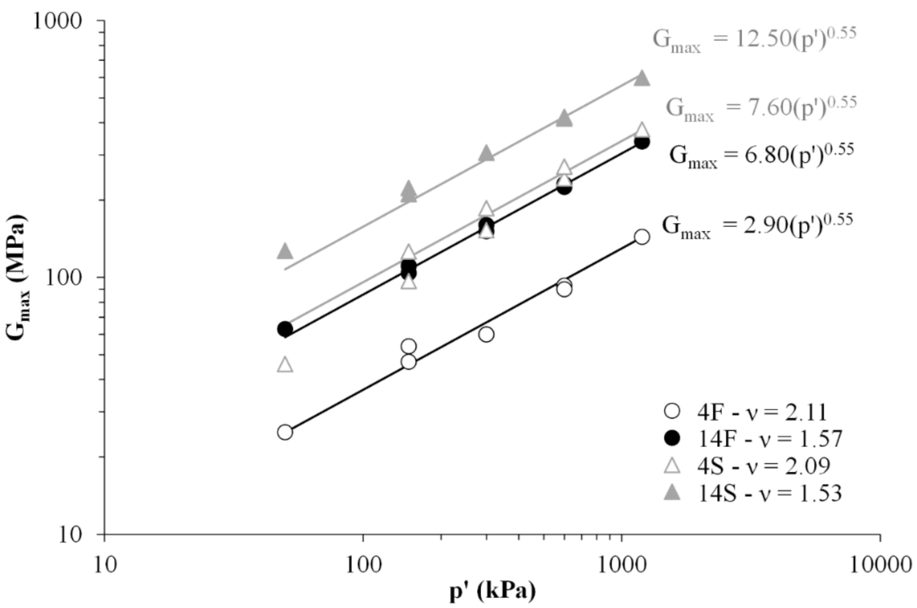

Figure 8 - Small-strain shear modulus against the mean effective confining pressure for flotation and slime tailings in loose and dense conditions.

3.2.3 Stress paths and critical states

The critical state is defined by the absence of variations of volume, deviatoric stress, and mean normal effective stress during the shearing of a soil/tailings. This state is generally achieved at large strain values [60]. From the results previously discussed, most specimens underwent volumetric compression during shearing and reached or were close to reaching this condition at the end of the shearing.

The stress paths of the iron ore tailings studied are presented in Fig. 9. The flotation tailings are shown in Fig. 9a and it can be seen that the endpoints of these triaxial tests define a unique CSL in q - p' space and the gradient of this line M_{tc} is 1.30 so the critical state angle of shearing resistance, φ'_{cs} is 32.2°. The stress paths of the slime tailings are shown in Fig. 9b and a unique CSL with a gradient M_{tc} of 1.35 is identified (φ'_{cs} = 33.4°).

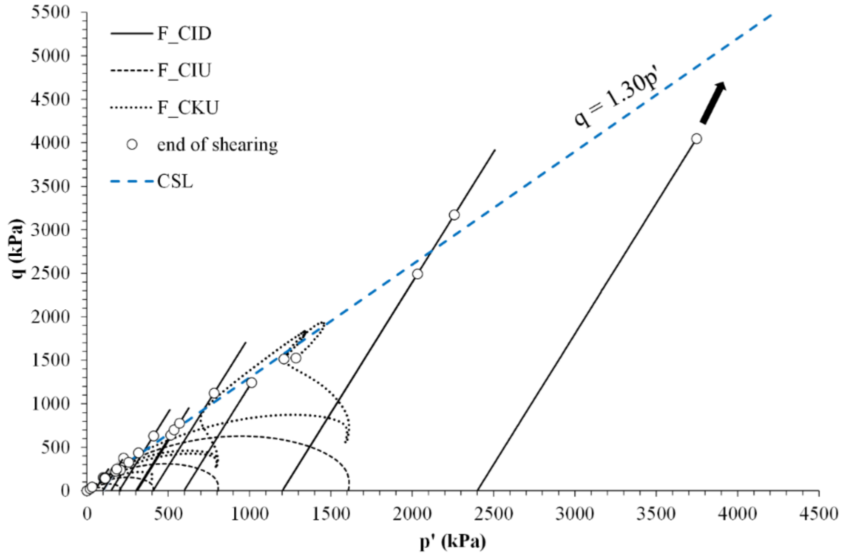

(a)

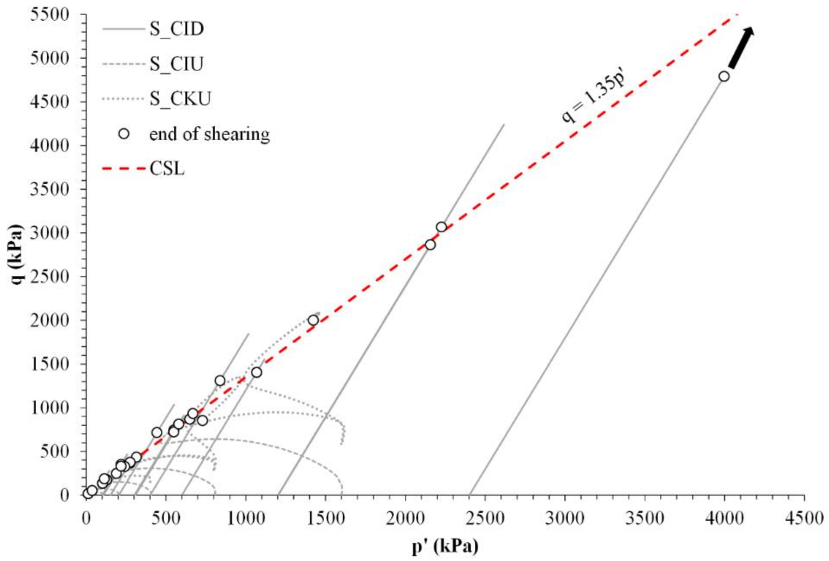

(b)

Figure 9 – Stress paths for triaxial tests for: (a) flotation tailings and (b) slime tailings.

The angle of shearing resistance at the critical state is principally controlled by grading, particle shape, and inter-particle sliding friction. Li et al. [2] compiled several types of tailings and concluded that all the φ'_{cs} values for different tailings fall into a narrow range at about 33° ± 2°, which indicates that the particle sizes and mineralogy do not affect much φ'_{cs}. The values obtained from the tailings of the present research are within the range indicated by Li et al. [2].

The difference between the critical state angle values for the different materials is minimal. These results are similar to the findings by Carrera et al. [14]. The authors found that the critical state angle varies only slightly for different sand-silt mixtures of the same tailings, probably due to the common origin of the materials. Several studies [61–64] performed DEM simulations to evaluate changes in critical states due to changing grading, with no reports of significant differences in the q-p' plane.

However, the small increase in φ'_{cs} with the increase in fines content might suggest a slightly greater strength for the finer material, possibly due to the interlocking portion as the fines provide a better packing or possibly the differences in mineralogy, and pure friction can be more related to their mineralogical origin. Some authors have also observed this difference in the critical state angle with grading changes. Chang et al. [65] reported critical state angles varying between 38.2° and 43.3° according to the grading variation of the material studied. Bedin et al.[41], testing Brazilian gold tailings, found a critical state angle of 33°, while Li et al. [2] found 34.8° for the same material with a finer grading.

Figure 10 is helpful to predict and confirm the chosen value of stress ratio at the critical state ($\eta = M_{tc}$) and verify which samples have effectively reached critical states. This is obtained by plotting the stress ratio (η) against the dilatancy rate for the drained tests or the stress ratio against the rate of change of excess pore-pressure ($\delta\Delta u/\delta\varepsilon_s$) for undrained tests. Following Cuccovillo and Coop [66] and Coop and Wilson [67], the dilatancy was calculated considering the total (plastic + elastic) volumetric and shear strain components. This is an adequate approach considering that the recoverable strain parcels are only relevant at the very beginning of the shear phase. Then, the M_{tc} value is observed at the intersection of the tests with the zero dilatancy (or pore pressure change) axis and the tests that reached this point had attained the critical state. Figure 10a presents the tests for flotation tailings with the M_{tc} of 1.30 and the Fig. 10b shows the tests for slime tailings with the M_{tc} of 1.35, which are in agreement with the values defined in the q-p' plane. The loose tests reached the defined values of M_{tc} while the dense ones are still tending towards this value.

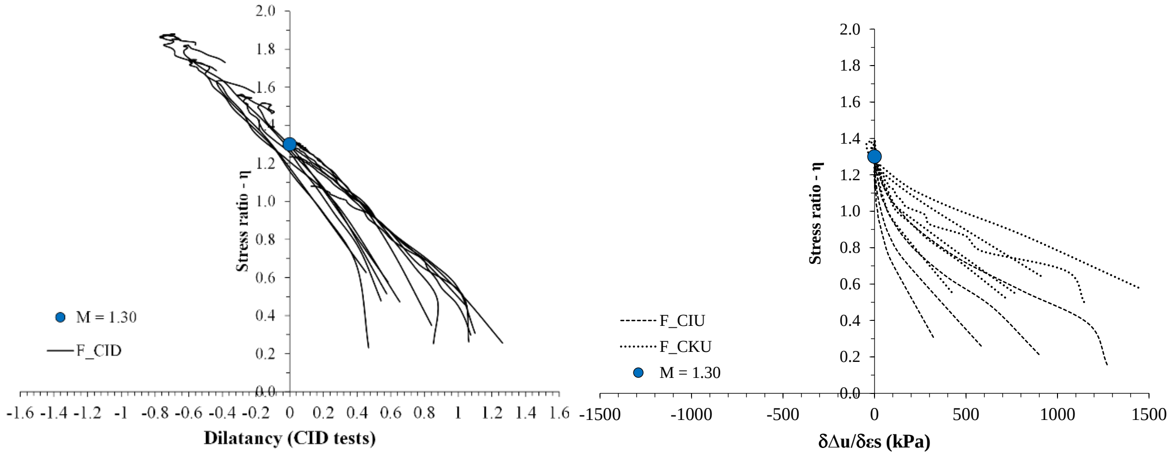

(a)

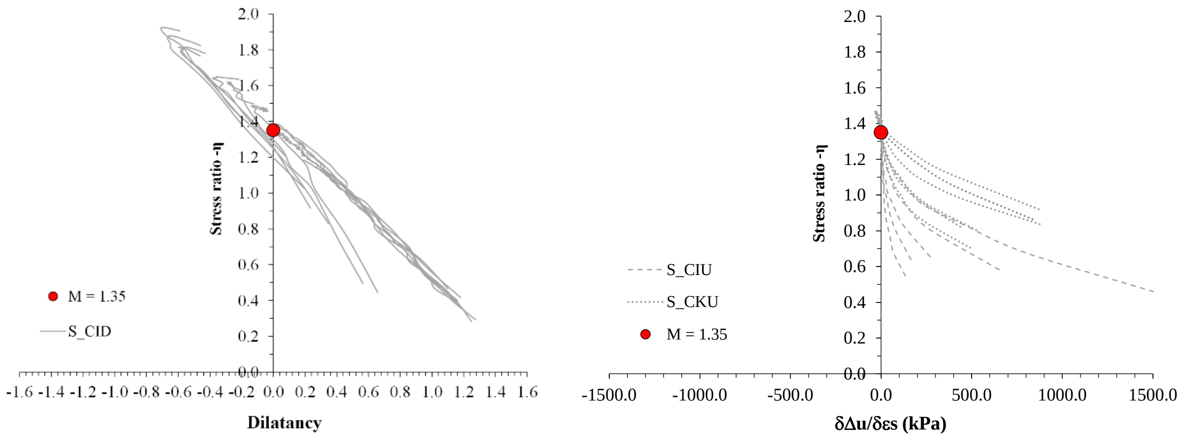

(b)

Figure 10 – Stress-dilatancy and stress-excess pore-pressure variation analysis for: (a) flotation tailings and (b) slime tailings.

Figure 11 plots the maximum stress ratio ($\eta = q/p'$) *versus* the minimal dilation rate ($D_{min} = d\varepsilon_v/d\varepsilon_s$) for the dense triaxial tests. Higher η values were reached for more dilatant specimens (denser specimens at lower confining pressures), while $\eta = M_{tc}$ is observed for specimens at critical state and with no dilatancy ($D_{min} = 0$). Despite some scatter, the points lie close to a linear fitting for both tailings, and the lines fitted are almost parallel with slight translation upwards for the tailings with higher fines content (S). This similarity again is due to their common origin and suggests a low influence of the grading and mineralogy on dilatancy and stress ratio, as previously observed.

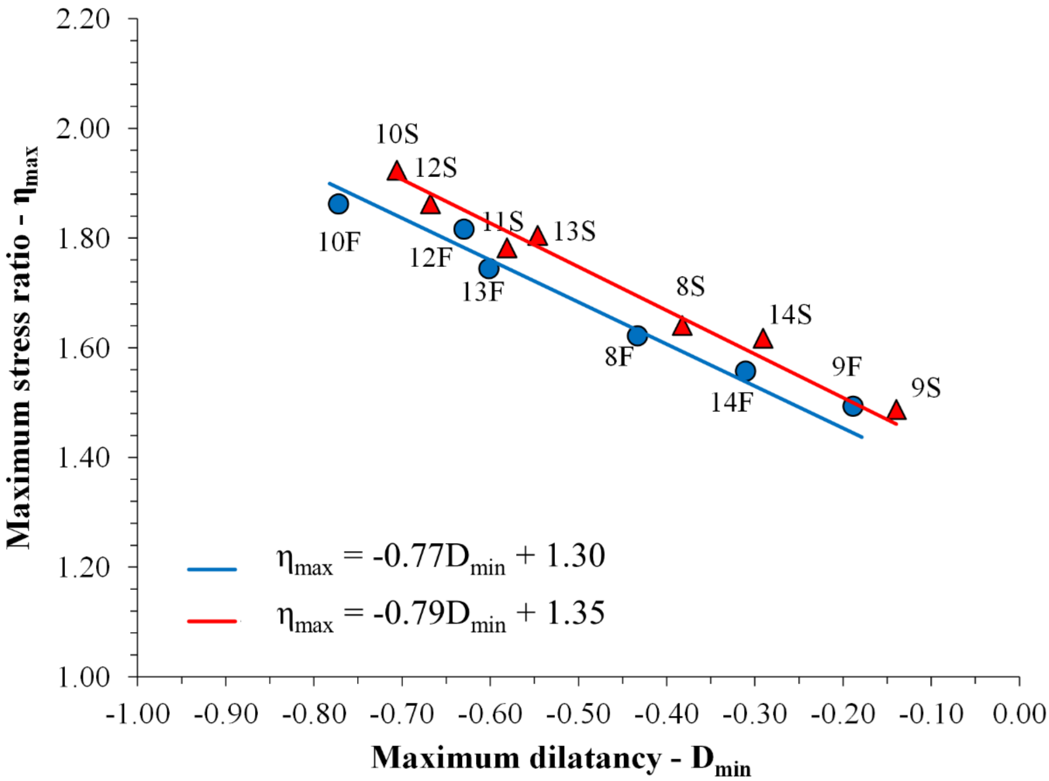

Figure 11 – Stress-dilatancy correlation.

The critical state line (CSL) in the $v - \ln p'$ plane was determined by the values of v and p' corresponding to the end of the tests which were identified to reach critical state. For both tailings tested, dense specimens could not be used in CSL fitting as they had not yet achieved constant volume and stress states and almost certainly suffered from significant strain localization. The curved CSLs fitted were obtained through a power-law shown in Equation (1) [68] which attempts to include all the stress range tested.

$$v = a - b \cdot ln(\frac{p'}{p'_{ref}})^c \quad (1)$$

where a refers to the curve intercept, b refers to the initial curve slope, c is the exponent that controls the curvature and p'_{ref} was chosen as 100 kPa.

This idealization allows representation of the curvature in the CSL, that is clear for both flotation (Fig. 12a) and slime tailings (Fig. 12b). Over the stress levels tested it was possible to achieve a unique CSL for both tailings, for the wide range of initial void ratios tested indicating the absence of a transitional mode of behavior on shearing. For three of the four initial densities tested herein, there is convergence to a unique CSL. However, Only the densest samples stay far with an upward movement towards the defined CSL, but this is more an artifact of incomplete testing and/or strain localization.

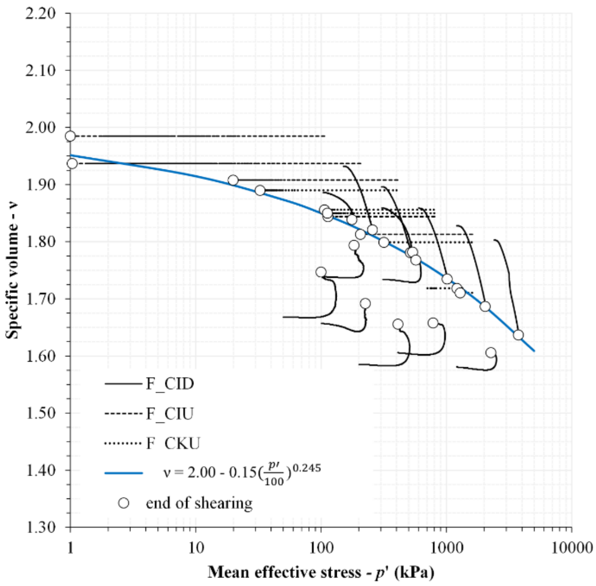

(a)

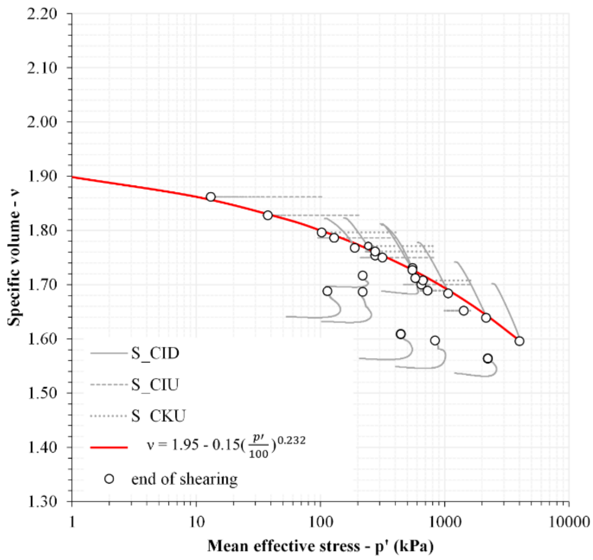

(b)

Figure 12 – Critical state line in the ν - ln p' plane for: (a) flotation tailings and (b) slime tailings.

The CSL defined for the slime tailings has the parameters a = 1.95, b = 0.15 and c = 0.232, while the adjustment to the CSL for flotation tailings gave a = 2.00, b = 0.15 and c = 0.245. The curves obtained have identical slopes, different exponents, and different intercepts, so the CSLs determined are almost parallel at low pressures with the intercept shifting downwards owing to the fabrics-related differences that end up affecting the intergranular stress distribution. Physically, non-plastic fines tend to fill the voids existing between larger grains and reduce the void ratio up to a point termed threshold fines content (TFC) after which the void ratio starts to increase because the increasing fines content tend to separate the larger particles [18, 69] . This ends up impacting the attainable maximum and minimum void ratio values and, thus, the location of the CSL. These findings agree with the behavior usually reported in the literature. Different authors [14, 18, 70] have also observed the translation of the curve with a change in fines content.

Bandini and Coop [71] suggest that the CSL movement with increasing fines is a result of both vertical translation and rotation. These effects can also be noted for the materials tested. As the stress level increases, the coarser material has a greater shift in gradient, while for the finer there is only a slight difference in CSL gradient. Thus, the final gradients of each tailings vary according to the fines content with a trend of convergence at higher pressures.

As also noted by Carrera et al. [14]although the different gradings have similar CSLs in the q-p' plane, in the $v - \ln p'$ plane they are significantly different at low pressures. The tendency of behavior was also explored at high pressure in this paper. Figure 13 shows the projection of the CSL for each tailing type compared with the unique isotropic NCL obtained. The endpoints of the shearing tests that reached the critical state are highlighted for each CSL. The two CSLs tend to converge at stresses around 30 MPa to a unique CSL parallel to the limiting NCL and with a spacing ratio (r) of 2.71. This value is similar to clays and also other non-plastic materials such as iron tailings (2.7 [72]), gold tailings (2.2 [2]) and copper tailings (3.3[72]) and is the quotient between the normal consolidation pressure (p'_0) and the corresponding pressure at the critical state line (p'_c) considering the same specific volume [73].

The behavior of both tailings with different gradings was found to converge at higher pressures to a unique NCL and CSL. This trend of convergence can also be noted in other experimental results found in the literature [2, 14], although the authors have not discussed it. These results suggest that changing the grading and mineralogy might not necessarily influence the critical state of the materials at very high pressures. At lower stress levels these two tailings are not strictly transitional, or at least it is a different class of transitional behavior. The compression curves are each non-unique, but the critical state is unique so that the strains imposed during compression cannot have been sufficient to reach a unique fabric but the shear and volumetric strains occurring during shearing to failure were. This contrasts with the soils investigated by Todisco and Coop [74] for which no volumetric or shear strains brought about unique volumes (and hence fabric) states in either compression or shear.

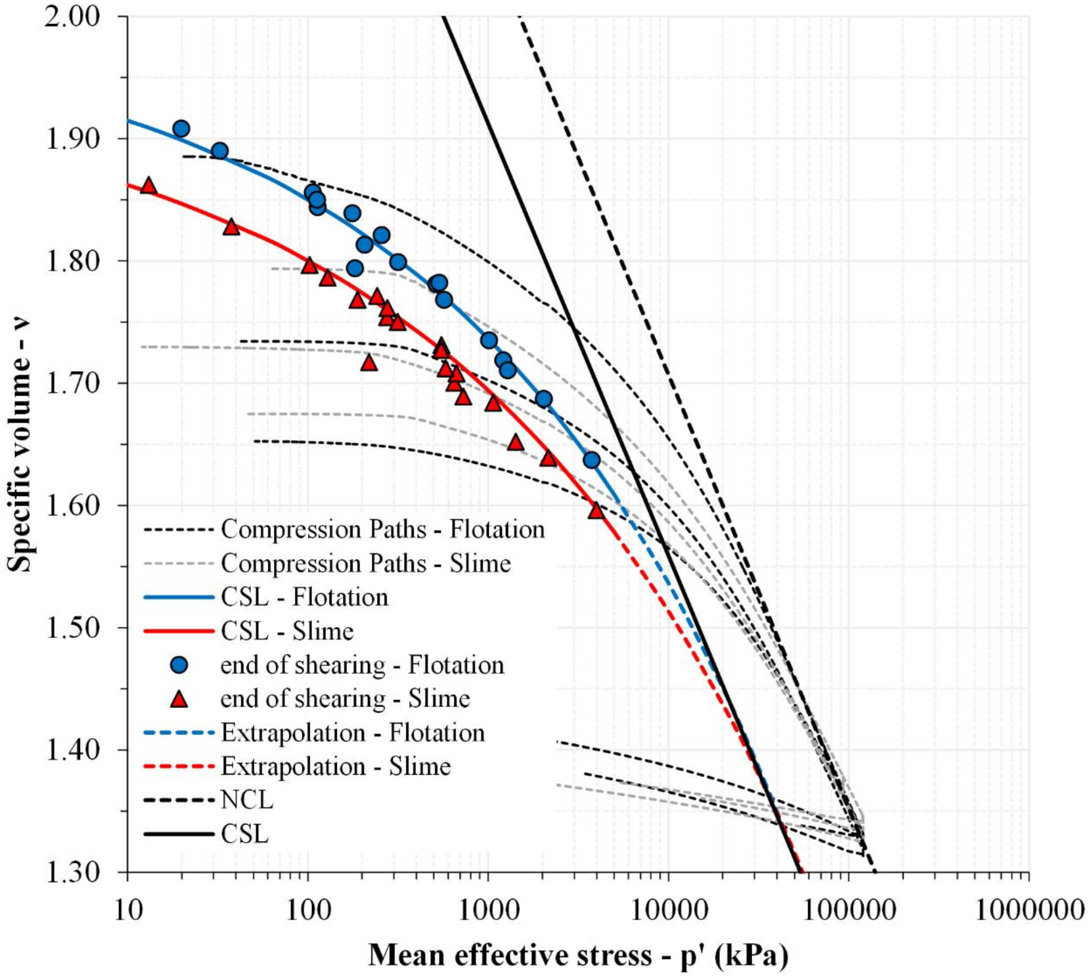

Figure 13 – CSLs and compression paths converging into unique CSL and NCL.

3.2.4 Liquefaction

The concept of liquefaction is approached in different ways in the literature, and it is often hard to understand which definition each author adopts. Herein, liquefaction is referred to the transformation of granular material from a solid state into a liquefied state due to increased pore-water pressure up to the achievement of a zero effective stress state, characterized by a complete loss of strength. Analogously, such a state can be termed a critical steady state with zero residual strength [75]. In this regard, the curved critical state line (flatter at lower stresses and parallel to the NCL at higher stresses) gives rise to a changing susceptibility to liquefaction as the stress level increases, as also noted by Li et al. [2] and Carrera et al. [14]. Bedin et al. [41] have defined different regions for curved CSL, indicating the changing susceptibility to liquefaction as stress level increases. The regions indicated are: (1) true liquefaction, which corresponds to low stresses and high specific volumes for which there is a complete loss of strength; (2) flow instability, which ranges from low to moderate stress with typical strain softening behavior and positive excess pore-pressure generation, which significantly reduces deviatoric stresses, but still, achieve steady states with a finite residual shear strength; (3) stable condition, drained and undrained critical states coincide and a stable slope essentially parallel to the NCL; and, (4) particle breakage, when the stresses reached are greater than those at the onset of shear-induced grain crushing.

Figure 14 shows examples of stress paths for different responses obtained during this research for flotation tailings (Fig. 14a) and slime tailings (Fig. 14b). Regarding flotation tailings, it is observed that tests 15F and 16F suffered a severe strain softening which has led to the complete loss of strength, characterizing a steady state with no residual strength (p' and q tends to zero). Tests 17F and 18F have also shown strain softening but reached an ultimate steady state in which the residual strength was different from zero. This is an indication that the complete loss of strength in an undrained response is not reached amongst all specimens whose states are lying above the CSL, as well as the susceptibility to it depends more on the initial void ratio than on the stress state of the soil.

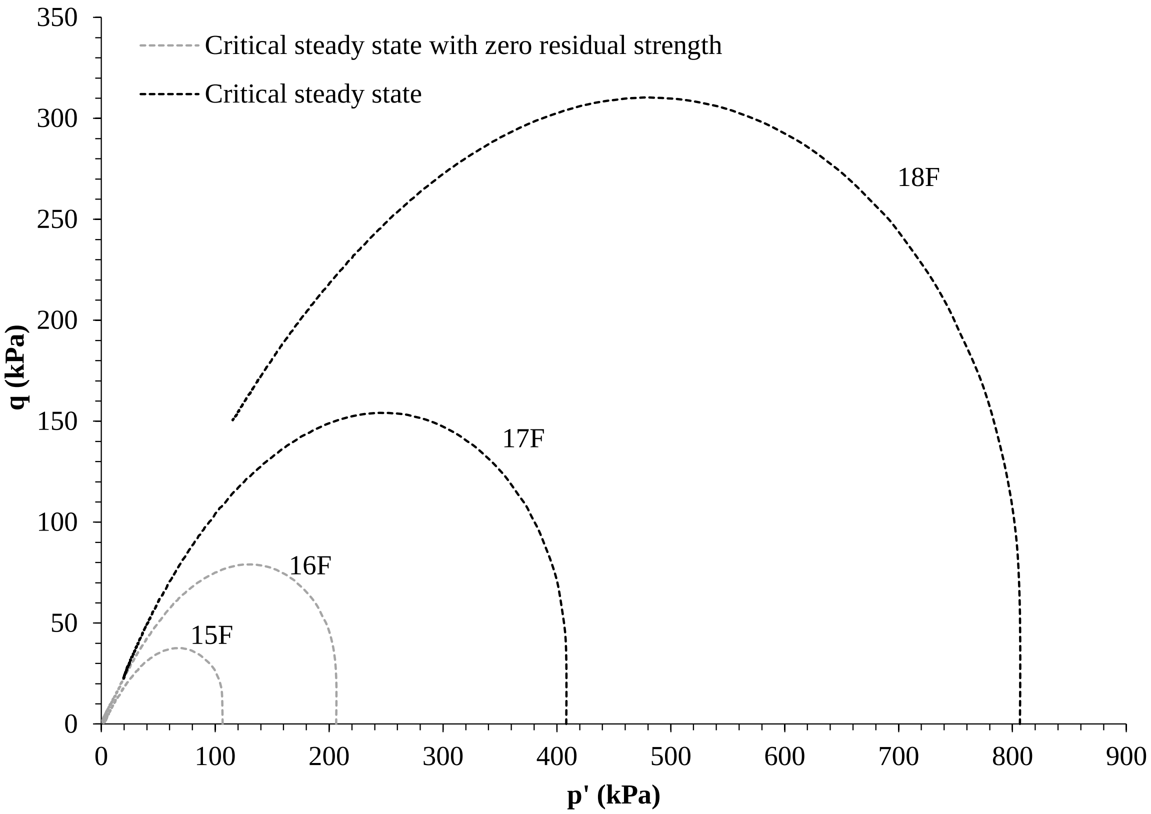

(a)

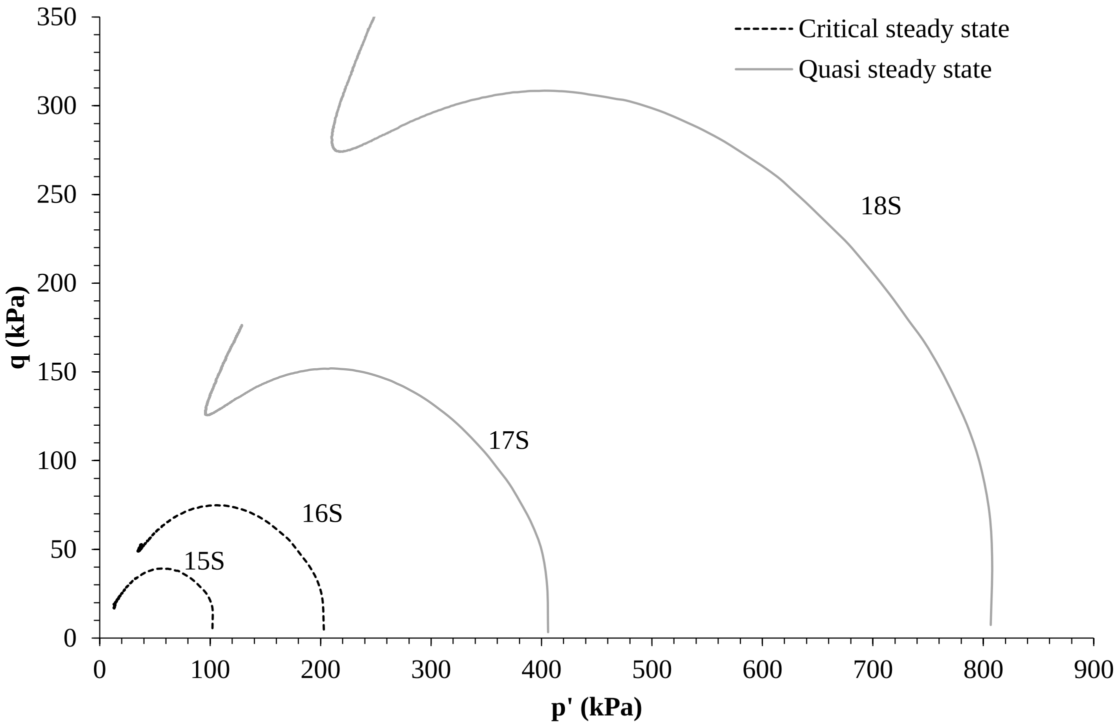

(b)

Figure 14 – Liquefaction analysis for: (a) flotation tailings and (b) slime tailings.

Considering the same tests on slime tailings, none has shown a complete loss of strength. Tests 15S and 16S have exhibited strain-softening that has led to a critical steady state with residual strength different from zero. At higher pressures, the tests (17S and 18S) presented a contractive behavior until a minimum mean effective stress or phase transformation was reached, with the pore water pressures increasing quickly, and then the behavior changed to a dilative trend. In other words, a quasi-steady state followed the phase-transformation point with subsequent strain-hardening. This trend has been reported by Li and Coop [20] in other tailings.

The complete loss of strength in undrained loading occurs when the initial state lies above the asymptote that exists for any CSL at lower stress levels, as is clearer for the flotation tailings (Fig. 12a). Nonetheless, Figure 13 shows that this asymptote is higher for the flotation tailings than the slimes, and given the e_{max} is similar for both tailings (Table 1) the slimes should therefore be more susceptible to liquefy. The fact that, it is the flotation tailings that are more prone to complete strength loss is due to the much higher initial specific volumes that were achieved for this material (Table 2) than for the slimes (Table 3) despite using similar preparation techniques. As well, the slime tailings lying above the CSL presented lower state parameter values, indicating a lower contractive trend than the flotation tailings.

4 Concluding remarks

The present research evaluated the mechanical response of two compacted filtered iron ore tailings from same origin but different gradings by means of drained and undrained triaxial tests. The following conclusions can be drawn:

- A unique Normal Compression Line (NCL) was determined for both tailings with different gradings and different initial densities when tested to stresses up to 120 MPa. However, there were almost parallel compression curves at lower stress levels, with compression paths that must be associated with differences in fabric corresponding to their initial void ratios. These results demonstrate that the deposition density affects the in-situ volume and compression behavior of the material, indicating a slowly convergent behavior for the typical stress levels used in dry stacks while a total convergence in shearing and compression was noticed only at very high stress levels;
- The grain size distribution was evaluated for looser and denser samples of each tailing type after being tested in isotropic stress to 120 MPa. It was found that there was no significant difference in the particle breakage for the flotation tailings due to differences in initial

density. Also, the slime tailings showed no particle breakage after the test which is probably related to the increased packing efficiency and coordination number resulting from the greater fines content of the sample compared to the flotation tailings that showed particle breakage;

- Both tailings showed a unique CSL in the *p'*-*q* plane. The flotation tailings have an M_{tc} of 1.30 with critical state friction angle φ'_{cs} of 32.2°, while the slime tailings had an M_{tc} of 1.35 and φ'_{cs} = 33.4°. The similar values indicate that the critical state angle depends mainly on the origin of the material and an increase in fines content changes this value only slightly. The slime tailings also had slightly larger values for the maximum stress ratios for the same dilatancy. This behavior may be related to better interlocking on slime tailings due to the presence of more fines between the sand grains;
- The critical state line (CSL) in the v – ln p' plane was fitted with a power-law with the parameters a = 1.95, b = 0.15 and c = 0.232 for the slime tailings and a = 2.00, b = 0.15 and c = 0.245 for the flotation tailings. The wide range of initial void ratios tested indicates the absence of transitional mode of behavior on shearing, even if the compression curves at lower stress levels are not unique. The CSLs of the two tailings have identical slopes, different exponents and different intercepts. They are almost parallel at low pressures with the intercept shifting downwards. As the stress level increases, the coarser material has a greater change in gradient, while for the finer there is a smaller difference in the CSL gradient.
- The projection of the NCLs and CSLs were considered up to high pressures. The curves for the CSLs showed tendency of convergence at high stresses to a unique CSL for both materials parallel to the limiting NCL and with spacing ratio of 2.71. This indicates that for these tailings the behavior at very high stresses is insensitive to the initial grading, density and mineralogy, while at lower stresses those factors affect the behavior significantly.
- Finally, the results reinforce the need for a broader investigation of different tailings at different initial states for application in dry stacks. Both the fines content and initial void ratio influenced the mechanical response of the tailings for usual pressures in engineering applications, being required extremely high pressures to achieve the classical critical state behavior for the materials studied. A better understanding of tailings behavior in its full range of possible states is therefore required to predict the performance of the projected Tailings Storage Facility.

Data availability statement: Some or all data, models, or code that support the findings of this study are available from the corresponding author upon reasonable request.

Funding: The authors wish to express their appreciation to VALE S.A., MEC/CAPES, and Brazilian Research Council (CNPq) for the support to the research group.

Declarations

Conflict of interest: The authors declare that they have no known competing financial interests or personal relationships that could have appeared to influence the work reported in this paper.

NOTATION

CSL	critical state line
CIU	isotropically consolidated undrained triaxial compression test
CID	isotropically consolidated drained triaxial compression test
CKU	K-consolidated undrained triaxial compression test
DEM	discrete element method
FC	fines content
F	flotation tailings
IOT	iron ore tailings
NCL	normal compression line
PI	plasticity index
QF	region of Quadrilátero Ferrífero
S	slime tailings
TFC	threshold fines content
D	dilation rate = $d\varepsilon_v/d\varepsilon_s$
D_{min}	maximum dilation rate
e	void ratio
e_0	void ratio prior to consolidation
e_{min}	minimum void ratio
e_{max}	maximum void ratio
G	elastic shear modulus
m	slope of convergence lines
M	critical state stress ratio
M_{tc}	critical state stress ratio at triaxial compression
ϕ_{cs}'	critical state friction angle
υ	specific volume = 1 + e
η	Stress ratio = q/p'
η_{max}	Top stress ratio = q/p'
p'	mean effective stress
p_0'	mean effective stress at the beginning of the shearing phase
q	deviatoric stress $(\sigma_1 - \sigma_3)$
σ'_1, σ'_3	principal effective stresses

σ'_{h} horizontal effective stresses

σ'_{v} vertical effective stresses

u pore water pressure

ε_a axial strain

ε_s shear strain

ε_v volumetric strain

w water content

w_L liquid limit

References

1. Statista (2022) Iron ore mine production in Brazil from 2015 to 202

2. Li W, Coop MR, Senetakis K, Schnaid F (2018) The mechanics of a silt-sized gold tailing. Engineering Geology 241:97–108. https://doi.org/10.1016/j.enggeo.2018.05.014

3. Kossoff D, Dubbin WE, Alfredsson M, et al (2014) Mine tailings dams: Characteristics, failure, environmental impacts, and remediation. Applied Geochemistry 51:229–245. https://doi.org/10.1016/j.apgeochem.2014.09.010

4. Xiaolong Z, Shiyu Z, Hui L, Yingliang Z (2021) Disposal of mine tailings via geopolymerization. Journal of Cleaner Production 284:124756. https://doi.org/10.1016/j.jclepro.2020.124756

5. Yin G, Li G, Wei Z, et al (2011) Stability analysis of a copper tailings dam via laboratory model tests: A Chinese case study. Minerals Engineering 24:122–130. https://doi.org/10.1016/j.mineng.2010.10.014

6. Yao C, Wu L, Yang J, et al (2021) Influences of tailings particle size on overtopping tailings dam failures. Mine Water Environ 40:174–188. https://doi.org/10.1007/s10230-020-00725-3

7. Islam K, Murakami S (2021) Global-scale impact analysis of mine tailings dam failures: 1915–2020. Global Environmental Change 70:102361. https://doi.org/10.1016/j.gloenvcha.2021.102361

8. WISE - Wise Uranium Project (2022) Chronology of major tailings dam failure

9. Olivier G, de Wit T, Brenguier F, et al (2018) Ambient noise Love wave tomography at a gold mine tailings storage facility. Géotechnique Letters 8:178–182. https://doi.org/10.1680/jgele.18.00016

10. Gomes RB, De Tomi G, Assis PS (2016) Iron ore tailings dry stacking in Pau Branco mine, Brazil. Journal of Materials Research and Technology 5:339–344. https://doi.org/10.1016/j.jmrt.2016.03.008

11. Consoli NC, Vogt JC, Silva JPS, et al (2022) Behaviour of compacted filtered iron ore tailings–Portland cement blends: New Brazilian trend for tailings disposal by stacking. Applied Sciences 12:836. https://doi.org/10.3390/app12020836

12. Davies M (2011) Filtered dry stacked tailings: The fundamentals. https://doi.org/10.14288/1.0107683

13. Santamarina JC, Torres-Cruz LA, Bachus RC (2019) Why coal ash and tailings dam disasters occur. Science 364:526–528. https://doi.org/10.1126/science.aax1927

14. Carrera A, Coop M, Lancellotta R (2011) Influence of grading on the mechanical behaviour of Stava tailings. Géotechnique 61:935–946. https://doi.org/10.1680/geot.9.P.009

15. Papadopoulou A, Tika T (2008) The effect of fines on critical state and liquefaction resistance characteristics of non-plastic silty sands. Soils and Foundations 48:713–725. https://doi.org/10.3208/sandf.48.713

16. Rahman MM, Lo SR (2008) The prediction of equivalent granular steady state line of loose sand with fines. Geomechanics and Geoengineering 3:179–190. https://doi.org/10.1080/17486020802206867

17. Zlatovic S, Ishihara K (1995) On the influence of nonplastic fines on residual strength. In: Proceedings of the 1st International Conference on Earthquake Geotechnical Engineering. AA Balkema, Tokyo, Japan, pp 293–244

18. Thevanayagam S, Shenthan T, Mohan S, Liang J (2002) Undrained fragility of clean sands, silty sands, and sandy silts. J Geotech Geoenviron Eng 128:849–859. https://doi.org/10.1061/(ASCE)1090-0241(2002)128:10(849)

19. Torres-Cruz LA, Santamarina JC (2020) The critical state line of nonplastic tailings. Can Geotech J 57:1508–1517. https://doi.org/10.1139/cgj-2019-0019

20. Li W, Coop MR (2019) Mechanical behaviour of Panzhihua iron tailings. Can Geotech J 56:420–435. https://doi.org/10.1139/cgj-2018-0032

21. Nocilla A, Coop MR, Colleselli F (2006) The mechanics of an Italian silt: An example of ‘transitional’ behaviour. Géotechnique 56:261–271. https://doi.org/10.1680/geot.2006.56.4.261

22. Shipton B, Coop MR (2015) Transitional behaviour in sands with plastic and non-plastic fines. Soils and Foundations 55:1–16. https://doi.org/10.1016/j.sandf.2014.12.001

23. Xu L, Coop MR (2017) The mechanics of a saturated silty loess with a transitional mode. Géotechnique 67:581–596. https://doi.org/10.1680/jgeot.16.P.128

24. Coop MR (2015) Limitations of a critical state framework applied to the behaviour of natural and “transitional” soils. In: Proceedings of the 6th International Symposium on Deformation Characteristics of Geomaterials. Buenos Aires

25. ASTM (2021) Test method for particle-size distribution (gradation) of fine-grained soils using the sedimentation (hydrometer) analysis - ASTM D7928. ASTM International

26. ASTM (2017) Test methods for liquid limit, plastic limit, and plasticity index of soils - ASTM D4318. ASTM International

27. ASTM (2014) Test methods for specific gravity of soil solids by water Pycnometer - ASTM D854. ASTM International

28. ASTM (2016) Test methods for minimum index density and unit weight of soils and calculation of relative density - ASTM D4254. ASTM International

29. ASTM (2017) Test methods for maximum index density and unit weight of soils using a vibratory table - ASTM D4253. ASTM International

30. ASTM (2021) Test methods for laboratory compaction characteristics of soil using standard effort (12,400 ft-lbf/ft^3 (600 kN-m/m^3)) - ASTM D698. ASTM International

31. ASTM (2021) Test methods for laboratory compaction characteristics of soil using modified effort (56,000 ft-lbf/ft^3 (2,700 kN-m/m^3)) - ASTM D1557. ASTM International

32. ASTM (2017) Practice for classification of soils for engineering purposes (Unified Soil Classification System) - ASTM D2487. ASTM International

33. ASTM (2020) Test s - ASTM D7181. ASTM Internationalmethod for consolidated drained triaxial compression test for soil

34. ASTM (2020) Test method for consolidated undrained triaxial compression test for cohesive soils - ASTM D4767. ASTM International

35. David Suits L, Sheahan T, Frost J, Park J-Y (2003) A critical assessment of the moist tamping technique. Geotech Test J 26:9850. https://doi.org/10.1520/GTJ11108J

36. Corrêa MM, Oliveira Filho WL (2019) Impact of methods used to reconstitute tailings specimens on the liquefaction potential assessment of tailings dams. REM, Int Eng J 72:507–513. https://doi.org/10.1590/0370-44672018720164

37. Das BM (2019) Advanced Soil mechanics, 5th ed. CRC Press, Boca Raton : Taylor & Francis.

38. Nakata Y, Hyodo M, Hyde AFL, et al (2001) Microscopic particle crushing of sand subjected to high pressure one-dimensional compression. Soils and Foundations 41:69–82. https://doi.org/10.3208/sandf.41.69

39. McDowell GR (2022) On the yielding and plastic compression of sand. Soils and Foundations 139–145

40. Altuhafi FN, Coop MR (2011) Changes to particle characteristics associated with the compression of sands. Géotechnique 61:459–471. https://doi.org/10.1680/geot.9.P.114

41. Bedin J, Schnaid F, Viana da Fonseca A, Costa Filho LDM (2012) Gold tailings liquefaction under critical state soil mechanics. Géotechnique 62:263–267. https://doi.org/10.1680/geot.10.P.037

42. Fukumoto T (1992) Particle breakage characteristics of granular soils. Soils and Foundations 32:26–40. https://doi.org/10.3208/sandf1972.32.26

43. Coop MR, Lee IK, Houlsby GT, Schofield AN (1992) The behaviour of granular soils at elevated stresses. In: Proceedings of the Wroth Memorial Symposium held at St Catherine's College. Thomas Telford, Oxford

44. Lade PV, Yamamuro JA, Bopp PA (1996) Significance of particle crushing in granular materials. J Geotech Engrg 122:309–316. https://doi.org/10.1061/(ASCE)0733-9410(1996)122:4(309)

45. Einav I (2007) Breakage mechanics—Part I: Theory. Journal of the Mechanics and Physics of Solids 55:1274–1297. https://doi.org/10.1016/j.jmps.2006.11.003

46. Einav I (2007) Breakage mechanics—Part II: Modelling granular materials. Journal of the Mechanics and Physics of Solids 55:1298–1320. https://doi.org/10.1016/j.jmps.2006.11.004

47. Vilhar G, Jovičić V, Coop MR (2013) The role of particle breakage in the mechanics of a non-plastic silty sand. Soils and Foundations 53:91–104. https://doi.org/10.1016/j.sandf.2012.12.006

48. Mun W, McCartney JS (2017) Roles of particle breakage and drainage in the isotropic compression of sand to high pressures. J Geotech Geoenviron Eng 143:04017071. https://doi.org/10.1061/(ASCE)GT.1943-5606.0001770

49. Hardin BO (1985) Crushing of soil particles. J Geotech Engrg 111:1177–1192. https://doi.org/10.1061/(ASCE)0733-9410(1985)111:10(1177)

50. Wood DM (2006) Geomaterials with changing grading: A route towards modelling. In: Geomechanics and Geotechnics of Particulate Media, 1st ed. CRC Press, London, p 538

51. Ponzoni E, Nocilla A, Coop MR, Colleselli F (2014) Identification and quantification of transitional modes of behaviour in sediments of Venice lagoon. Géotechnique 64:694–708. https://doi.org/10.1680/geot.13.P.166

52. La Rochelle P, Leroueil S, Trak B, et al (1988) Observational approach to membrane and area corrections in triaxial tests. In: Donaghe R, Chaney R, Silver M (eds) Advanced Triaxial Testing of Soil and Rock. ASTM International, 100 Barr Harbor Drive, PO Box C700, West Conshohocken, PA 19428-2959, pp 715-715–17

53. Jefferies M (2022) On the fundamental nature of the state parameter. Géotechnique 72:1082–1091. https://doi.org/10.1680/jgeot.20.P.228

54. Been K, Jefferies MG (1985) A state parameter for sands. Géotechnique 35:99–112. https://doi.org/10.1680/geot.1985.35.2.99

55. Been K, Jefferies MG, Hachey J (1991) The critical state of sands. Géotechnique 41:365–381. https://doi.org/10.1680/geot.1991.41.3.365

56. Rahman MdM, Lo SR (2014) Undrained behavior of sand-fines mixtures and their state parameter. J Geotech Geoenviron Eng 140:04014036. https://doi.org/10.1061/(ASCE)GT.1943-5606.0001115

57. Santamarina JC, Klein KA, Fam MA (2001) Soils and waves. J. Wiley & Sons, Chichester ; New York

58. Cascante G, Santamarina JC (1996) Interparticle contact behavior and wave propagation. J Geotech Engrg 122:831–839. https://doi.org/10.1061/(ASCE)0733-9410(1996)122:10(831)

59. Cha M, Santamarina JC, Kim H-S, Cho G-C (2014) Small-strain stiffness, shear-wave velocity, and soil compressibility. J Geotech Geoenviron Eng 140:06014011. https://doi.org/10.1061/(ASCE)GT.1943-5606.0001157

60. Schofield A, Wroth CP (1968) Critical state soil mechanics. McGraw Hill, New Yorl

61. Muir Wood D, Maeda K (2008) Changing grading of soil: effect on critical states. Acta Geotech 3:3–14. https://doi.org/10.1007/s11440-007-0041-0

62. Yan WM, Dong J (2011) Effect of particle grading on the response of an idealized granular assemblage. Int J Geomech 11:276–285. https://doi.org/10.1061/(ASCE)GM.1943-5622.0000085

63. Li G, Liu Y-J, Dano C, Hicher P-Y (2015) Grading-dependent behavior of granular materials: from discrete to continuous modeling. J Eng Mech 141:04014172. https://doi.org/10.1061/(ASCE)EM.1943-7889.0000866

64. Ciantia MO, Arroyo M, O'Sullivan C, et al (2019) Grading evolution and critical state in a discrete numerical model of Fontainebleau sand. Géotechnique 69:1–15. https://doi.org/10.1680/jgeot.17.P.023

65. Chang N, Heymann G, Clayton C (2011) The effect of fabric on the behaviour of gold tailings. Géotechnique 61:187–197. https://doi.org/10.1680/geot.9.P.066

66. Cuccovillo T, Coop MR (1999) On the mechanics of structured sands. Géotechnique 49:741–760. https://doi.org/10.1680/geot.1999.49.6.741

67. Coop MR, Willson SM (2003) Behavior of hydrocarbon reservoir sands and sandstones. J Geotech Geoenviron Eng 129:1010–1019. https://doi.org/10.1061/(ASCE)1090-0241(2003)129:11(1010)

68. Jefferies M, Been K (2015) Soil liquefaction: A critical state approach, Second Edition, 0 ed. CRC Press

69. Chaney R, Demars K, Lade P, et al (1998) Effects of non-plastic fines on minimum and maximum void ratios of sand. Geotech Test J 21:336. https://doi.org/10.1520/GTJ11373J

70. Fourie AB, Blight GE, Papageorgiou G (2001) Static liquefaction as a possible explanation for the Merriespruit tailings dam failure. Can Geotech J 38:707–719. https://doi.org/10.1139/t00-112

71. Bandini V, Coop MR (2011) The influence of particle breakage on the location of the critical state line of sands. Soils and Foundations 51:591–600. https://doi.org/10.3208/sandf.51.591

72. Li W (2017) The mechanical behavour of tailings. City University of Hong Kong

73. Yu H-S, Zhuang P-Z, Mo P-Q (2019) A unified critical state model for geomaterials with an application to tunnelling. Journal of Rock Mechanics and Geotechnical Engineering 11:464–480. https://doi.org/10.1016/j.jrmge.2018.09.004

74. Todisco MC, Coop MR (2019) Quantifying "transitional" soil behaviour. Soils and Foundations 59:2070–2082. https://doi.org/10.1016/j.sandf.2019.11.014

75. Yoshimine M, Ishihara K (1998) Flow Potential of sand during liquefaction. Soils and Foundations 38:189–198. https://doi.org/10.3208/sandf.38.3_189